ENGINEERING BACTERIAL GLYCOBIOLOGY FOR THE CREATION OF GLYCOCONJUGATE VACCINES

A Dissertation
Presented to the Faculty of the Graduate School
of Cornell University
In Partial Fulfillment of the Requirements for the Degree of
Doctor of Philosophy

by

Taylor Currie Stevenson

Cornell University, January 2017

ENGINEERING BACTERIAL GLYCOBIOLOGY FOR THE CREATION OF GLYCOCONJUGATE VACCINES

Taylor Currie Stevenson, Ph. D.

Cornell University 2017

The use of vaccines has led to the effective eradication of several human diseases which were once epidemic such as smallpox and polio. Vaccines have also dramatically decreased the incidence of other diseases including rabies, mumps, and measles. A common theme to these diseases is that their etiological pathogens are viruses. In general, it has proven to be a much more challenging task to develop effective vaccines against bacterial pathogens. The field of bacterial vaccinology has seen success in recent decades with the development of glycoconjugate vaccines. A canonical glycoconjugate vaccine uses polysaccharides isolated from bacterial pathogens and chemically conjugates them to strong protein antigens, thus allowing the immune system to generate a robust and long lasting immune response against a component of the pathogen that is an ideal target for immune system. This approach has been very successful against some bacterial pathogens including *Heamophilus influenzae*, *Streptococcus pneumoniae,* and *Salmonella enterica*. However, the semi-synthetic process for making these glycoconjugates is lengthy, requiring several rounds of purification before and after conjugation chemistry links protein to polysaccharide.

This work will discuss alternative wholly biosynthetic processes for the creation of glycoconjugate vaccines. I have done preliminary work engineering the glycobiology of *Escherichia coli* to display azide-linked sugars on lipid-linked oligosaccharides with the overall

goal of performing *in vivo N*-linked protein glycosylation to create glycoprotein vaccines that can be functionalized through well-characterized bioorthogonal chemistry. I was able to observe the presence of these azide-linked sugars on the outer membrane of *E. coli* by fluorescence based screening in a flow cytometer. Additionally, I have leveraged the use of recombinant outer membrane vesicles (OMVs) combined with *in vivo* and *in vitro* bacterial *N*-linked glycosylation to formulate new glycoconjugate vaccines against the bacterial pathogen *Francisella tularensis*. The presence of these glycoproteins in and on the OMVs was verified through Western blotting, proteinase protection assays, and density gradient ultracentrifugation.

I have also formulated a non-canonical glycoconjugate vaccine by producing OMVs coated in the common bacterial extra-cellular polysaccharide poly-*N*-acetylglucosamine (PNAG). I have shown that these PNAG OMVs are able to elicit a strong, class-switched glycan-specific antibody response against PNAG in mice. Mice vaccinated with these PNAG OMVs are partially protected against lethal challenge with *Staphylococcus aureus* (8/16 survivors in PNAG OMV immunized mice as compared to 3/16 survivors in PBS control mice). I have also shown that sera from mice immunized with PNAG OMVs has bactericidal activity against the attenuated strain *F. tularensis* LVS, suggesting mice immunized with PNAG OMVs may be protected from a wide range of pathogens. These studies provide several routes for novel formulation of glycoconjugate vaccines against bacterial pathogens.

BIOGRAPHICAL SKETCH

Taylor Currie Stevenson was born in New Orleans, Louisiana in the summer of 1988 to Dr. Paula Currie and Mark Stevenson. One baby brother (Zachary Stevenson), seven years, and six to seven house floods later, his family moved to Hammond, LA where Taylor began his schooling in the Ponchatoula public school system. In 2004, he applied and was accepted to the Louisiana School for Mathematics, Sciences, and Arts where he finished his junior and senior years of high school. During this time, he began his scientific inquiries in the lab of Dr. Michael Doughty at Southeastern Louisiana University. After graduating from LSMSA with distinction in 2006, Taylor began his tenure at Rice University in Houston, Texas. He graduated from Rice in 2010 after completing a B.S. in Biochemistry and Cell Biology and a B.A. in Computational and Applied Mathematics. During his time at Rice, Taylor completed an honors thesis working in the laboratory of Dr. Jonathan “Joff” Silberg, and participated in the founding of the Rice IGEM team. As a member of the Rice IGEM team, he was a team leader for the project titled “BioBeer: A resveratrol producing yeast for brewing beer”. Taylor was accepted into the Biomedical Engineering Ph.D. program at Cornell University where he joined the DeLisa Research Group.

I dedicate this work to my loving parents, Mark Stevenson and Paula Currie. Their patience with, and support of, my interests and endeavors are a big part of my success. I'd also like to recognize my younger brother, Zachary Stevenson. Zack, thanks for understanding my early departure from home and your patience with helping me learn how to drive years after I should have figured it out on my own. I'd also like to thank the many influential teachers and mentors who helped nurture my interest in scientific discovery: Mrs. and Dr. Hynes at LSMSA; Dr. Michael Doughty at SLU; Drs. Jonathan Silberg, Oleg Igoshin, Steven Cox, and Mark Embree at Rice University. Finally, I'd like to thank my many friends, who believed in me even when I did not. I'm at my best when trying to live up to your images of me.

ACKNOWLEDGEMENTS

The most important acknowledgement I must offer is to Dr. Matthew DeLisa, my mentor during the last six years of graduate school. Matt, thanks for helping me focus a vague interest in glycobiology and vaccinology into this collection of works. I extend my thanks to all the members of the DeLisa Research Group for their help with experimental design and strategy. I'd especially like to thank Drs. Linxiao Chen and Jenny Valentine along with Emily Perregeux for their collaborations and independent contributions to the space of glycOMVs. To all of you, your support and input have been critical to the conception and execution of the projects in this dissertation.

I'd also like to acknowledge my other committee members: Dr. Yung-Fu Chang for his endless positivity and help with establishing and carrying out the animal trials discussed in this work and Dr. David Putnam for making sure I knew my stuff during both my A and B exams. I'd also like to acknowledge Dr. Gerald Pier for his offered ideas and materials in collaboration with us on the PNAG OMV vaccine project. Additionally, I'd like to thank Drs. Daniel Dube and Benjamin Lundgren for their generously provided materials and bacterial strains used during the azide labeling project.

This work was partially supported by the National Science Foundation Graduate Research Fellowship Program.

TABLE OF CONTENTS

LIST OF FIGURES

LIST OF TABLES

CHAPTER 1

INTRODUCTION: GLYCOBIOLOGY AND ITS IMPLICATION FOR VACCINE DEVELOPMENT

Introduction

Vaccines are recognized as one of the most significant advances in medical history. They have led to the eradication of several diseases in areas where they were once endemic. Despite these great strides, effective vaccines against a variety of bacterial pathogens remain elusive[1]. The advancement of biochemical and genetic engineering techniques led to development of targeted subunit vaccines that contain a minimal subset of pathogen derived biomolecules[2]. Of these subunit vaccines, glycoconjugate subunit vaccines containing a pathogen sourced oligosaccharide antigen chemically conjugated to an adjuvant carrier have recently risen to prominence as vaccine candidates against bacterial pathogens[3-5]. Unfortunately, these glycoconjugate vaccines are often difficult to produce or fail to elicit a protective immune response[6]. There is a clear need for better ways of formulating and producing more effective glycoconjugate vaccines.

The discovery that the bacterium *Campylobacter jejuni* is capable of producing N-linked glycoproteins caused an explosion in the field of prokaryotic glycobiology and subsequent development of new vaccine production technologies[7]. One of the biggest boons to this endeavor was the functional transfer of the *C. jejuni* protein glycosylation locus (*pgl*) into *Escherichia coli*[8]. This recombinant pathway can glycosylate many different proteins with a wide variety of oligosaccharides in an easy to culture, and genetically tractable, laboratory strain of bacteria[9-11]. Additionally, this reaction has been successfully reconstituted *in vitro*, allowing for cell free production of glycoproteins from recombinant bacterial source[12]. The

three different components of the canonical bacterial N-linked protein glycosylation reaction are the target protein to be glycosylated, the lipid-linked oligosaccharide (LLO), and the oligosaccharyltransferase (OST). By supplying these components *in vivo* or *in vitro*, it is possible to efficiently produce N-linked glycoproteins that contain oligosaccharide antigens from different pathogens. **In this work, I will discuss engineering bacterial glycobiology to produce different LLO subunits to be used as substrates in N-linked glycosylation reactions both *in vivo* and *in vitro* with the aim of formulating new vaccine candidates.**

It has previously been shown by the DeLisa Research Group and others that outer membrane vesicles (OMVs) from Gram-negative bacteria can elicit a strong antigen specific immune response to protein and oligosaccharide antigens present in, and displayed on, OMVs [13-16]. These observations provide an alternative approach to formulating glycoconjugate vaccines. Whereas traditional approaches require the conjugation of an oligosaccharide antigen to a carrier protein, we have observed a strong protective immune response to recombinant oligosaccharide antigens displayed on OMVs. Fortunately, purification of OMVs is relatively simple when compared to purification of semisynthetic or biosynthetic glycoproteins. Additionally, OMVs are strong stimulators of the innate immune system, potentially making the immune response stimulated by them more protective and longer lasting than the response generated by traditional glycoconjugates[17-20]. These features make recombinant OMVs an attractive platform for vaccine development. **In this work, we discuss how recombinant OMVs produced from a hypervesiculating strain of *E. coli* engineered to produce the bacterial polysaccharide antigen poly-*N*-acetylglucosamine (PNAG) protect mice against lethal**

challenge with *Staphylococcus aureus* and PNAG specific antibodies produced by those mice have *in vitro* bactericidal activity against *Francisella tularensis* LVS.

Bacterial Glycobiology

Bacterial glycobiology is a field that has existed since the early days of bacteriology. When Hans Gram first stained the peptidoglycan of bacterial cells in a heterogeneous sample, a fundamental classification of bacterial species based on their divergent membrane structure and underlying glycobiology became apparent. Bacterial glycobiology has since led to further understanding of bacterial components from peptidoglycan common in all species to the more esoteric capsular polysaccharides of Gram-positive species and the lipopolysaccharides (LPS) produced by Gram-negative bacteria. Investigation into these extracellular polysaccharides has led to a better understanding of bacterial carbohydrate metabolism, environmental colonization, and host-pathogen interactions. In this introduction, I will briefly discuss the metabolism of glycobiology and how bacteria use sugars as both sword and shield against their environments.

In the world of carbohydrate catabolism, glucose is king. In metabolic networks, it is the entry point of the glycolysis pathway, one of the most ancient and ubiquitous of all metabolic pathways. Bacteria like *E. coli* have evolved to make use of this pathway and can transport glucose into cells using the phosphotransferase system (PTS). These transporters are so named because they phosphorylate their substrates as the substrates are being transported into the cell. This phosphorylation primes the glucose molecule for entry into the glycolysis pathway and prevents its subsequent diffusion out of the cell. One glucose molecule is broken down during

glycolysis into two pyruvate molecules, generating two adenosine triphosphates (ATPs) and two reduced nicotinamide adenine dinucleotides (NADHs) to be used as energetic currency in other cellular processes. This catabolic pathway is always necessary, and often sufficient, for the energy requirements of bacteria. In the case of the laboratory strain *Escherichia coli* K-12, a facultative aerobe capable of catabolizing a wide range of substrates, glucose and glycolysis is so preferred that the presence of glucose serves as a global repressor for other catabolic pathways. In a phenomenon termed the "glucose effect", if there is enough glucose being transported through the PTS, *E. coli* will not use any other substrate as an energy source. It will even eschew the much more efficient citric acid cycle and subsequent oxidative phosphorylation, which can produce approximately 36 ATPs per glucose molecule. Additionally, this catabolite repression keeps the metabolism of the cell balanced toward anabolic processes, allowing for rapid growth and accumulation of biomass. In contrast, as the catabolic pathways tend to converge at the metabolic nodes associated with the early steps of glycolysis, the anabolic pathways tend to diverge from these same few metabolic nodes.

Different anabolic carbohydrate products can serve a wide variety of functions in a bacterial cell such as integral structural components, protective barriers against diffusion or attack, colonization of different environments, and modulation of host-specific immune responses. A major node in the metabolic network of these anabolic pathways is the metabolite *N*-acetylglucosamine (GlcNAc). The biosynthetic pathway of GlcNAc in *E. coli* begins with the synthesis of glucosamine-6-P (GlcN-6-P) from intracellular pools of the glycolysis metabolite fructose-6-P and the amino acid glutamine via the enzyme GlmS. The activated GlcN-6-P is then isomerized by GlmM into GlcN-1-P. The next two steps in the process are catalyzed by the

enzyme GlmU, a protein comprised of two separate functional domains. The C-terminal domain of GlmU catalyzes the addition of the acetyl group onto the C1 amine from acetyl-CoA onto GlcN-1-P, forming GlcNAc-1-P, while the N-terminal domain catalyzes the addition of uridine diphosphate (UDP) from uridine triphosphate (UTP) forming GlcNAc-UDP. This activated form of GlcNAc funnels directly into the production of peptidoglycan, polysaccharides, and glycolipids.

If *E. coli* is not in an environment where glucose is plentiful, a plethora of metabolic pathways become active as the cell begins to evaluate its environment for alternative growth substrates. The previously discussed acetylated hexosamine, GlcNAc, is one such substrate capable of sustaining growth in *E. coli*. As GlcNAc is a major component of the rigid structural material peptidoglycan, it is available for use every time a cell must break down peptidoglycan prior to undergoing division. When peptidoglycan in the cell wall is degraded, subunits are transported into the cell via the permease AmpG and broken down into its constituents by AmpD, releasing free cytosolic GlcNAc. The free GlcNAc is then phosphorylated by NagK into GlcNAc-6-P, whereupon it can enter the biosynthetic pathway as though it had been produced by GlmS. All the proteins involved in the recycling of GlcNAc from peptidoglycan are expressed constitutively. However, when the glucose PTS becomes less active as glucose is depleted in the environment and extracellular concentrations of GlcNAc are high enough to warrant its use as an energy source, the *nagEBACD* catabolic operon becomes active. The *nagE* gene in this operon codes for a GlcNAc PTS that allows the cell to efficiently transport and phosphorylate extracellular GlcNAc to form GlcNAc-6-P. The enzymes NagA and NagB from this operon are then able to funnel GlcNAc-6-P into glycolysis by converting it to fructose-6-P through deacetylation and deaminization, respectively. The metabolic balance between anabolism and

catabolism is partially maintained by the transcription factor NagC, which acts as a repressor for the *nagEBACD* operon when GlcN-6-P levels are low in the cell. As GlcN-6-P levels rise within the cell, not only does NagC repression of the *nagEBACD* operon lessen, but NagC also acts an activator of transcription for the GlmS and GlmU proteins in the anabolic pathways for GlcNAc. This simultaneous transcription of the catabolic *nagEBACD* and the anabolic *glmUS* operons seems to create a futile cycle. This futile cycle is avoided by post-translational modification of the isomerase GlmM, which is only active when it is phosphorylated under conditions that are favorable for growth. It is this enzyme which acts to direct flux of GlcNAc pathway toward either catabolism and fructose-6-P or anabolism and UDP-GlcNAc based on the conditions within the cell. If GlcNAc is indeed being shunted toward anabolic pathways, it is likely fated to end up in either peptidoglycan or LPS. Alternatively, it can be acted upon by a variety of epimerases which can change the identity of the hexose component (i.e. from UDP-GlcNAc to UDP-ManNAc) before being used as a substrate for a glycosyl transferase.

Peptidoglycan and LPS synthesis in *E. coli* begins on the inner leaflet of the cytoplasmic membrane. Undecaprenyl pyrophosphate (UPP), or bactoprenol, is a common lipid carrier for carbohydrates in bacteria. Activated sugars such as UDP-GlcNAc are added to it by glycosyltransferases which function in a processive manner to construct carbohydrate oligomers, also known as glycans. Once these glycans are fully assembled, they can be recognized by specific flippases which flip the lipid-linked oligosaccharide (LLO) so that the oligosaccharide portion is facing the periplasm. Once flipped, the glycan, or glycopeptide, conjugated lipid can be used in either peptidoglycan synthesis or the O-antigen component of LPS.

The LPS of Gram-negative bacteria consist of three major components: a hexa-acylated disaccharide of keto-deoxyoctulosonate (lipid A), a highly-conserved oligosaccharide (inner and outer cores), and a repeating oligosaccharide subunit (O-antigen). Lipid A is a strong stimulator of the innate immune system due to its ability to trigger an inflammatory response through the activation of TLR4, earning it the name endotoxin. The O-antigen structure can vary widely, even among the same species of bacteria, adding to the many serotypes within a bacterial species. Though most laboratory strains of *E. coli* lack the ability to produce an O-antigen due a deletion in the *rfb* gene cluster, they can still produce Lipid A conjugated to a "core oligosaccharide" which is synthesized and transported to the pathway through a different mechanism[21]. Restoration of O-antigen synthesis can be achieved by supplying the missing *E. coli* genes. Interestingly, if an exogenous O-antigen biosynthetic pathway from a different Gram-negative species is transformed into an *E. coli* strain deficient in O-antigen synthesis, it will produce an O-antigen with a structure that is highly similar to the donor species [9]. The glycan subunit built on UPP in the cytoplasm by glycosyltransferases gets flipped to the periplasm and acted on by the polymerase Wzy which creates linear polymers of varying length. The polymers of various length are then conjugated onto lipid A by the WaaL ligase before the mature LPS molecule is transported to the outer membrane where it decorates the cell surface.

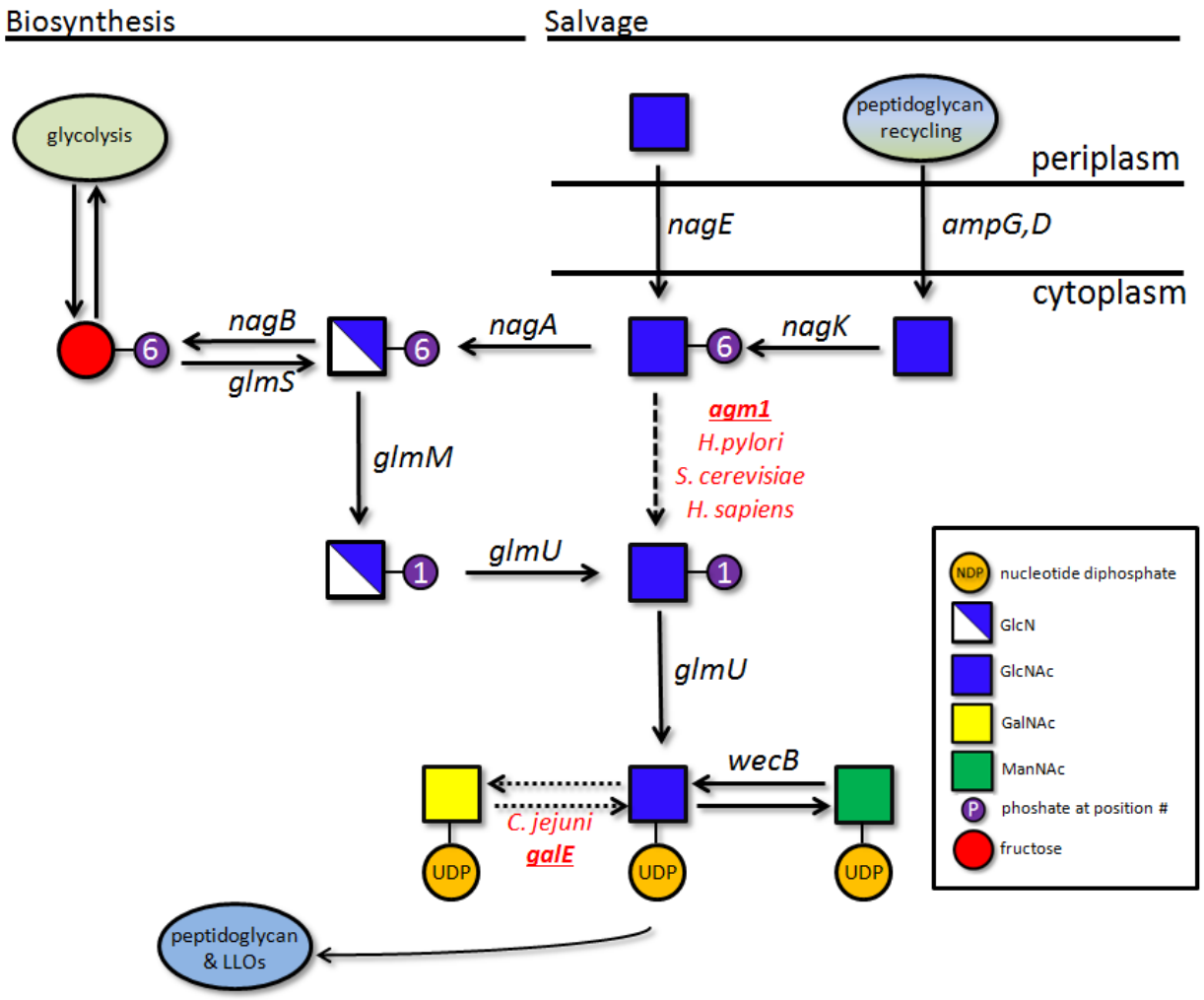

Figure 1.1: *N*-acetylglucosamine (GlcNAc) metabolism in *E. coli*. Metabolic scheme showing the metabolism of glucosamine in a typical laboratory strain of *E. coli*. The figure is divided into the biosynthesis (left) and salvage (right) pathways for glucosamine (GlcN). When GlcNAc is being catabolized or recycled, it is imported into the cell through either the NagE transporter or AmpG,D complex, respectively. If imported through AmpG,D, it must first be phosphorylated by NagK before entering the catabolic pathway catalyzed by NagA,B which feeds directly into glycolysis. The lower portion shows the anabolic pathway for activated UDP-GlcNAc through which either biosynthesized or salvaged GlcN-6-P is shuttled. Notice that *E. coli* lacks an *agm1* homolog (present in the listed species) that allows for direct salvage of GlcNAc. Once formed, UDP-GlcNAc can be acted upon by epimerases to generate a wide variety of activated *N*-acetylhexosamines for use in various biosynthetic pathways including peptidoglycan and LPS.

N-linked protein glycosylation in bacteria

Bacterial glycobiology garnered new attention when *N*-linked protein glycosylation was discovered in bacteria. Specifically, the pathogen *Campylobacter jejuni* was shown to produce N-linked glycoproteins by research in 1999[7]. In a system that is like the N-linked glycosylation pathway in eukaryotic cells, lipid linked oligosaccharides are transferred onto acceptor proteins in the periplasm by an oligosaccharyltransferase (OST). The prokaryotic OST (PglB) is a single subunit that is most analogous to the Stt3 subunit in the eukaryotic OST complex. Instead of the dolichol linked glycans of the eukaryotic system, *C. jejuni* PglB takes advantage of the periplasmic UPP-linked oligosaccharides by transferring the glycan *en bloc* to an acceptor protein. Like the eukaryotic OST complex, the *C. jejuni* PglB has a specific acceptor sequon that contains the asparagine to be glycosylated. Specifically, it is the five amino acid sequence D/E-X_1-*N*-X_2-S/T where X_1 and X_2 are any amino acids except proline. This is a more stringent requirement than that of the eukaryotic acceptor sequence which is less strict at only three amino acids N-Y-S/T [22, 23]. Numerous studies have shown that the sequence which is glycosylated most efficiently by *C. jejuni* PglB is DQNA[22]. This observation led to the development of the so-called "4xGlyc tag", a series of four repeating DQNAT sequences separated by serine linkers[11]. This new tag, which could easily be added to the terminal sequence of a protein, facilitated easy engineering of novel glycoproteins in *E. coli*.

The recombinant *pgl* locus has been used in *E. coli* to transfer the *C. jejuni* heptasaccharide to a wide variety of target proteins from small monomeric proteins like single chain variable fragments (scFvs) to large secretory toxins like Cholera toxin's B subunit (CtxB) and even integral membrane proteins such as cytolysin A (ClyA)[10, 22, 24]. In addition to

being able to transfer glycans onto many different classes of protein, PglB has also been able to transfer a wide range of glycans onto those proteins. The list of glycans includes the native *C. jejuni* heptasaccharide, the O-antigens of several Gram-negative species such as *F. tularensis*, and eukaryotic glycans such as the trimannosyl core glycan and the tumor associated T antigen[9, 10, 24, 25]. Despite its apparent flexibility for different protein and LLO substrates, PglB is limited by its rigid acceptor sequence and by the requirement that the glycan to be transferred has an N-acetylhexosamine as its first residue. Work has been done to generate mutated PglBs that have an altered sequence specificity and no longer require an N-acetylhexosamine as the base sugar [26]. These modified PglBs have been used to transfer novel glycans such as *Salmonella enterica* O-antigen onto acceptor proteins, and they have been used to glycosylate previously intractable targets that are glycosylated in mammalian systems but not in bacterial. The ability to transfer any UPP linked glycan onto any target or carrier protein, or protein glycan coupling technology (PGCT), has provided a powerful tool for the biosynthesis of glycoconjugates including glycoconjugate vaccine[9, 10, 26-28]. Though this method of producing glycoconjugates is both attractive and elegant in that it is complete biosynthesis of protein glycoconjugates without any downstream processing, its implementation is not always straightforward. First, PGCT requires the successful identification and transfer of a glycan biosynthetic pathway into *E. coli*, which can be time consuming depending on how well understood the biosynthetic pathway is. Additionally, the glycan biosynthetic pathway must be relatively orthogonal to endogenous glycobiology. The heterologous pathway starts with a readily available metabolite(s) in *E. coli* and can reproduce the recombinant glycan authentically. In an even more undesirable scenario, it may be that a

clear biosynthetic pathway for the desired glycan doesn't exist, requiring the researcher to engineer a novel pathway. Finally, though the path to purified glycoconjugates produced from PGCT is much clearer than for glycoconjugates produced by traditional semi-synthetic chemistry, a purification of glycoprotein from other cellular components is still required.

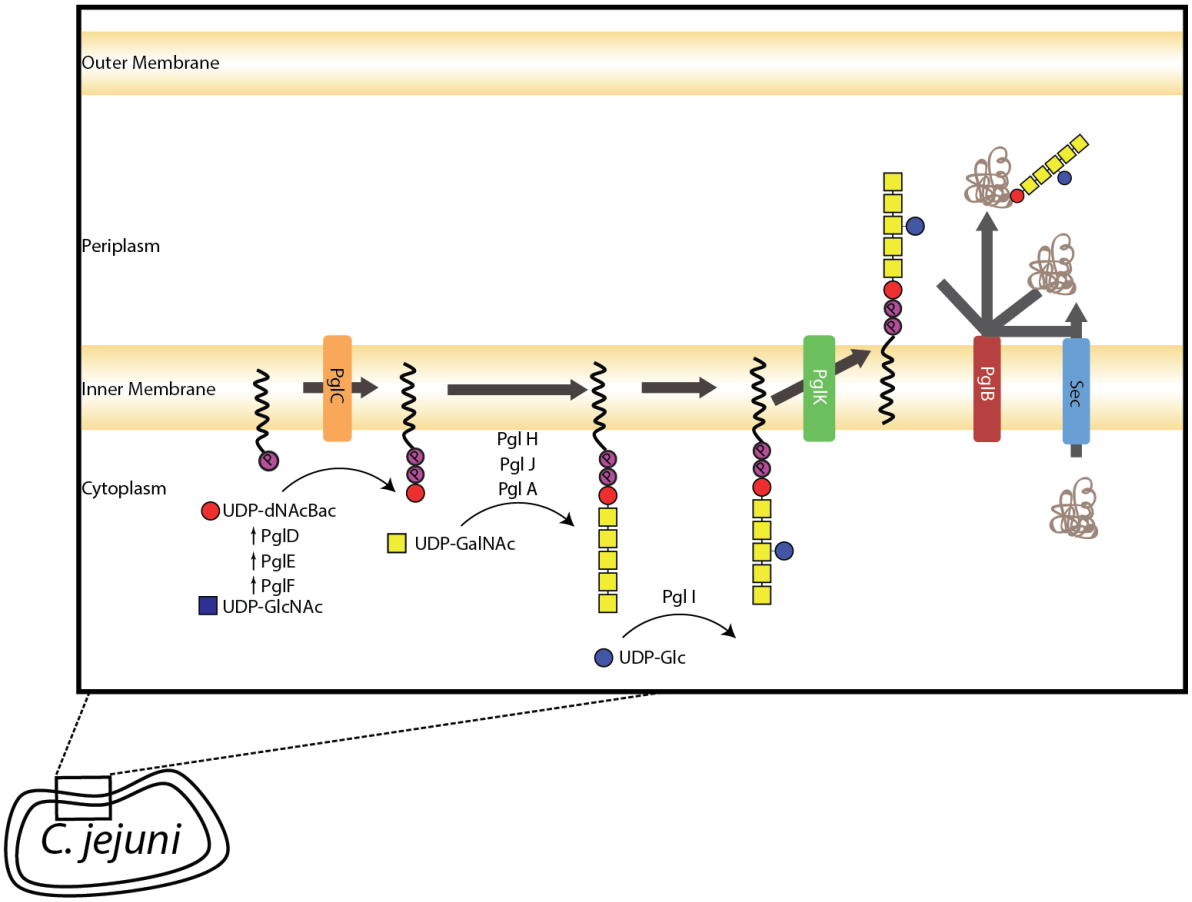

Figure 1.2: Bacterial *N*-linked protein glycosylation via the *C. jejuni pgl* pathway. This cartoon illustrates how the genes of the *pgl* locus use common metabolites such as UDP-GlcNAc to construct the unique heptasaccharide glycan. Notice the di-N-acetylbacillosamine (UDP-dNAcBac) as the first sugar being placed on UPP. If *pglD* is inactivated, dNAcBac is replaced by the more common GlcNAc as the first sugar residue [23]. The three components of the protein glycosylation reaction come together on the right-hand side of the cartoon. These three components (LLO, OST, and target protein) can be combined *in vitro* to carry out the protein glycosylation reaction. Not shown is PglG, as it plays no role in protein glycosylation[29].

Vaccine Immunology

Vaccines are one of the greatest advances in the history of medical science. They have been used to effectively eradicate several diseases including smallpox and polio, and they have dramatically decreased the incidence of other diseases including rabies, mumps, and measles. The modern vaccine formulations for these previously listed diseases have changed little from their historical formulations. Each of these vaccines is comprised of either an attenuated or killed sample of the pathogen responsible. The body's response to these vaccines is very similar to its response to the actual pathogen. The killed or attenuated pathogens contain many pathogen-associated molecular patterns (PAMPs) including LLOs and CpG DNA that are recognized by elements of the innate immune system including Toll-like receptors. Exposure to these PAMPs causes rapid production and release of immunostimulatory and inflammatory cytokines that recruit professional Antigen Presenting Cells (APCs) such as dendritic cells (DCs) to the site of exposure [30]. The recruited APCs then phagocytose the attenuated or killed pathogen and display digested peptide fragments from the pathogens on major histocompatibility complexes (MHCs). These APCs then bring the antigen fragments displayed on MHCII back to lymph nodes where naïve T-cells and B-cells are exposed to antigen. How these naïve cells respond to antigens presented on MHCs depends on the naïve cell type and the class of MHC presenting it [31].

Naïve B-cells with B-cell receptors (BCRs) that are specific to the antigen internalize it. Classically, antigens that are endocytosed by professional APCs are processed in lysosomes and loaded onto MHC class II complexes. Naïve $CD4^+$ T-cells are also exposed to the processed antigen presented on MHCII, and if their T-cell receptors (TCRs) are specific to the antigen, they

too will proliferate and differentiate into effector T-cells. When a B-cell that is displaying an antigen on MHCII encounters a cognate $CD4^+$ T-cell, there is a co-stimulation of proliferation and differentiation in both the T-cell and B-cell that leads to clonal selection of both cells and subsequent differentiation into plasma cells and effector helper T-cell [31]. This interaction results in production of high titers of class switched antibodies and is generally directed toward and effective against extracellular pathogens such as *Staphylococcus aureus*, *Streptococcus pyogenes*, *Neisseria meningitidis*, and *Yersinia pestis*.

Whereas MHCII generally displays peptides from exogenous antigens that are endocytosed by professional APCs, MHC class I displays endogenous antigens that are degraded in the cytoplasm. Unlike MHCII, which is generally only present on professional APCs, MHCI is present on almost every nucleated cell. Endogenously produced proteins are degraded within the cytosol and retroactively transported into the ER where the peptide fragments are loaded onto MHCI before being exported to the surface. In this way, MHCI functions as a reporter for aberrant protein production within cells such as when the cell is infected with a virus. If APCs become infected with a virus, they will also express viral proteins which are processed and displayed on MHCIs. When these infected APCs encounter naïve $CD8^+$ T-cells with TCRs that are specific to the viral antigens, the $CD8^+$ T-cells proliferate and differentiate to become cytotoxic T-cells (TCs). If these TCs encounter the same antigen presented by MHCI on other cells, the TCs induce apoptosis of the infected cell. Production of these TCs is generally known as the cellular immune response and is generally directed toward intracellular pathogens [31].

Though all cells have the potential to display endogenous antigens on MHCI, it has been observed that DCs can “cross present” exogenously translated proteins on MHCI [32, 33].

Through a poorly understood mechanism that involves retrograde vesicular transport and/or fusion of the vesicle with the endoplasmic reticulum, DCs have been shown to process exogenous protein antigens and display them on MHCI [34]. It is in this way that a non-viable viral particle or a component of an intracellular pathogen in a vaccine is able to elicit a relevant TC immune response that leads to death of infected cells [35].

Though the adaptive immune response to protein antigens is well understood, our conception of how the immune system responds to non-classical antigens such as LLOs or polysaccharides is still changing. The immune system can generate a glycan specific immune response through the previously described canonical method through one of two ways. First, if the glycan component of a glycoconjugate protein is recognized by a BCR, the entire protein can be endocytosed, processed, and displayed on MHCII, allowing for clonal expansion of the naïve B- cell and production of glycan specific antibodies[36, 37]. Second, if the glycan recognized by a naïve BCR is zwitterionic, once it has been endocytosed, the glycan can fit into the peptide binding cleft and be directly displayed on MHCII, allowing for clonal expansion of the B-cell and the glycan specific T-cell[38, 39]. There are, however, cases where class-switched glycan specific antibodies are produced when neither of the above two conditions are satisfied[15, 16]. How these glycans elicit such a strong humoral immune response is still poorly understood.

It is known that APCs can display LLOs to T-cells through presentation on CD1, allowing for progression of an immune response similar to that observed during classical peptide antigen display[37]. It is also possible for LLO or polysaccharide antigens to raise a humoral immune response through T-cell independent activation of naïve B-cells [40]. B-cells can be activated

and undergo proliferation, antibody class switching, and differentiation into plasma cells if the BCRs on naïve B-cells undergoes antigen mediated oligomerization in conjunction with strong immunostimulatory signals. This type of activation occurs when BCR binds to repeating subunits that are regularly spaced near each other. The repeating subunits of PS and LPS antigens makes them ideal antigens for this type of B-cell activation if they are co-administered with strong stimulators of the innate immune system [41].

Outer Membrane Vesicle Vaccines

Outer membrane vesicles (OMVs) are naturally produced liposomes that bleb off from Gram-negative bacteria. Their membrane composition is very like that of bacterial outer membranes and they range in size from approximately 50-250nm in diameter. They display integral outer membrane proteins, glycolipids, and polysaccharides on their outer surface. The lumen of OMVs contains periplasmic components including soluble proteins and peptidoglycan [42, 43]. The biological functions of OMVs are manifold and include moderation of membrane stress through shedding, transportation of soluble toxins or virulence factors during pathogenesis, and modulation of the host immune response during colonization [17, 44-49]. The extraction and recovery of OMVs is relatively straightforward, requiring two rounds of centrifugation separated by sterile filtration[42, 43, 50].

It has previously been shown by the DeLisa Research Group and others that OMVs have a potent immunostimulatory effect due to the many PAMPs in their composition [44, 45, 51, 52]. Additionally, OMVs contain many of the antigenic peptides and glycolipids that are often critical to developing an effective immune response to infection by Gram-negative bacteria. It

is for these reasons that OMVs are attractive candidates for vaccines against Gram-negative bacteria. Unfortunately, it is hard to obtain significant quantities of OMVs from pathogens as they are often difficult to culture at high density and the constitutive rate of OMV production can be quite low. Additionally, naturally derived OMVs tend to contain a large amount of LPS which can cause sepsis [53]. To overcome these limitations of native OMVs in current methods, the outer membrane of a Gram-negative bacterial pathogen is often partially solubilized with detergents to form OMVs. These harvested OMVs have modified lipid compositions that do not contain LPS, making them much less reactogenic. This was the approach taken during the recent development of the multi-subunit vaccine against *Neisseria meningitidis* type B[54]. Some of the downsides to this approach are that it is costly and that it can exclude some naturally occurring antigens from the OMVs such as O-antigens displayed on LPS. Additionally, it does not overcome the challenge of having to culture the pathogen of interest at high densities.

An alternative approach to generating OMVs for vaccines is through the use of recombinant OMV technology which allows us to express relevant antigens from pathogens in a non-pathogenic Gram-negative host such as *E. coli.* By targeting glycolipids and integral membrane protein antigens to the outer membrane and by localizing soluble antigens to the periplasm, it is possible to create recombinant OMVs with heterologously expressed antigens from pathogens [13, 14, 43, 55]. In addition, it is possible to induce hypervesiculation in *E. coli* without affecting cell viability via genetic knockouts [14, 50]. It is also possible to make recombinant OMVs from strains of *E. coli* that have modified LPS structure so that the lipid A portion of the molecules are much less reactogenic[56]. Thus, it is possible for recombinant

OMVs produced in *E. coli* to overcome the challenges presented by using native OMVs from pathogens. Recombinant OMVs produced from hypervesiculating strains of *E. coli* have been used to successfully immunize animals with a variety of antigens including glycans [13, 14].

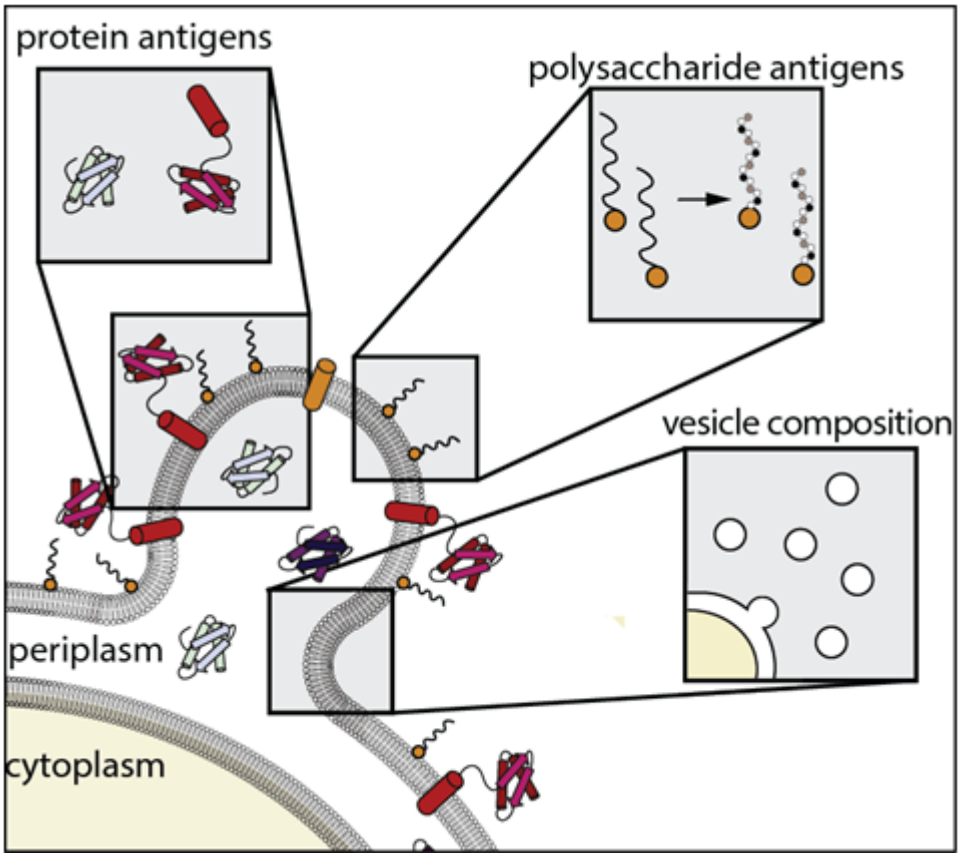

Figure 1.3: Engineering capability of recombinant OMV vaccines. OMVs have been engineered for vaccine development in several ways. Strains of *E. coli* have been made to hypervesiculate though genetic deletion of genes such as *tolR,A*, and *nlpI* (Kuehn, 2006). Recombinant protein antigens can be targeted to the surface of the OMVs through fusion with outer membrane proteins or to the lumen of OMVs through targeting to the periplasm (Rosenthal, 2014). Any glycoengineering that of extracellular polysaccharides affects glycans on the OMVs, allowing for delivery of carbohydrate antigens (Chen, 2016). Additionally, OMVs can be produced from strains of *E. coli* with modified lipid A structure, decreasing their reactogenicity (Chen, 2016).

CHAPTER 2

INCORPORATING BIOORTHOGONAL SUGARS INTO *E. COLI* LLOS

Introduction

Bioorthogonal chemistry is the study of reactions that do not interfere with normal biological processes and are thus "orthogonal" to them. It has become a useful tool for labeling specific metabolic products in living cells. An example of bioorthogonal chemistry in biology is the incorporation on non-canonical or chemically modified amino acids to create novel products form a synthetic biology approach and as an investigative tool in developmental biology[57-67]. The incorporation of novel amino acids into proteins structures is relatively straightforward as protein biosynthesis is a well-known and template-driven process[66]. In contrast, the use bioorthogonal chemistry in glycobiology can be more difficult in glycobiology as it is a much less mature field and the production of glycans is much more stochastic than the template driven processes of protein biosynthesis. Additionally, as carbohydrates are the primary source of energy for cellular metabolism, it is likely that any chemically modified sugars will be degraded by a cell as a matter of course. These challenges for bioorthogonal chemistry in glycobiology must be taken into consideration when developing methods for its use.

Carolyn Bertozzi and others have developed a method for chemically labeling glycans in living cells using bioorthogonal chemistry [58]. Their method takes advantage of the bioorthogonal reaction discovered in 1919 known as the Staudinger reaction[68]. The reaction occurs between a phosphine and an azide to produce an aza-ylide intermediate which normally would hydrolyze in water to form a primary amine and a phosphine oxide. However, if the aza-ylide forms with a nearby electrophilic trap and appropriate leaving group, water can facilitate

the formation of an amide bind between the two molecules, resulting in a Staudinger ligation (**Figure 2.1a**)[58]. This reaction is bioorthogonal and biocompatible in that neither the azide or phosphine groups interact significantly with biomolecules and that this reaction occurs in water under physiological condidtions. The Bertozzi group found that acetylated azide labeled sugars (azidosugars) are readily incorporated along with endogenous sugars using anabolic pathways, facilitating the labeling of a wide variety of cells types with phosphine-labeled fluorophores. This method facilitated the study of developmental biology and glycobiology in living organisms (**Figure 2.1a**)[62-64]. More recently, Danielle Dube has used similar methods to study bacterial glycobiology in *Helicobacter pylori*[69]. In this chapter, I will discuss the metabolic engineering of *E. coli* to allow for similar labeling *E. coli* glycans and demonstrate that labeling via flow cytometry (**Figure 2.1b)**.

Results

I have previously discussed hexosamine glycobiology in *E. coli* (**Figure 1.1**). Specifically, while *E. coli* is capable of internalizing GlcNAc, it must first be broken down to GlcN-6-P before it can be used in anabolic pathways. This lack of a direct salvage pathway for GlcNAc precludes the use of azide-labeled GlcNAc (GlcNAZ) in *E. coli*. The required metabolic modifications to facilitate the use of GlcNAZ are outlined in **Figure 2.1b**. First, the catabolic pathway for GlcNAc was deleted via knockout of the *nagA* gene. Second, a pathway for the direct conversion of GlcNAc-6-P to UDP-GlcNAc was created by the addition of two genes from *S. cerevisiae*, *agm1* and *uap1*. The gene *agm1* encodes a phosphoacetylglucosamine mutase which converts GlcNAc-6-P to GlcNAc-1-P, and *uap1* is a UDP-N-acetylhexosamine pyrophosphorylase which

then converts GlcNAc-1-P to UDP-GlcNAc. The endogenous *E. coli* gene, *glmU* could theoretically also provide this activity, but as it is a two-subunit protein with two distinct catalytic activities and substrate binding affinities, we theorized adding an enzyme with specialized activity (*uap1*) would result in better incorporation of GlcNAZ.

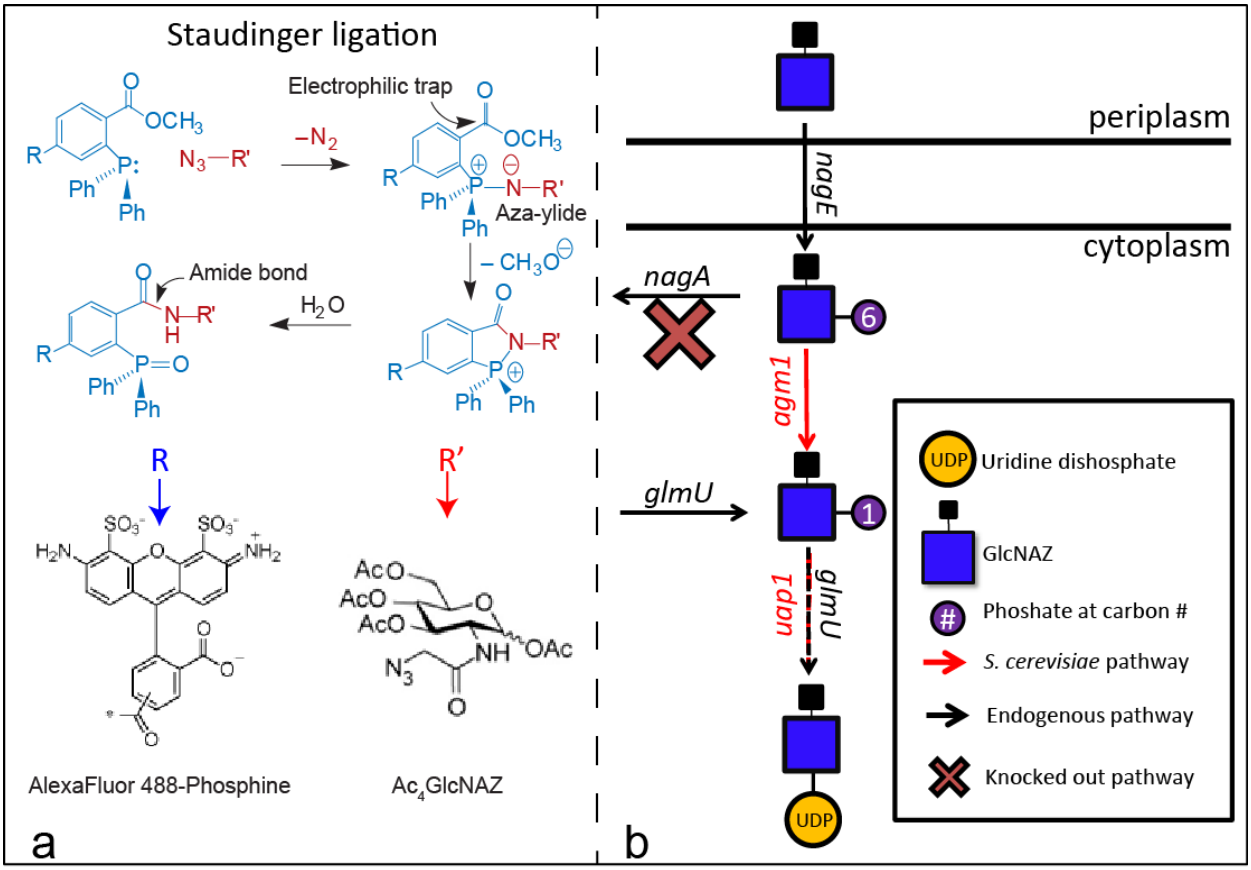

Figure 2.1: Staudinger ligation and engineered GlcNAZ salvage pathway. The left panel (**a**) shows the mechanism of the Stuadinger ligation and the two reactants used in this study, tetra-acetylated GlcNAZ and the fluorophore AlexaFluor 488-Phosphine (Saxon and Bertozzi, 2000). The right panel (**b**) shows the engineered salvage pathway for GlcNAc that the facilitates the use of GlcNAZ in *E. coli*. The black arrows and gene names are endogenous to *E. coli* while the red arrows and genes are from *S. cerevisiae* and are heterologously expressed. The red/black hatched arrow shows a reaction that is facilitated by both endogenous and heterologous genes.

A strain of *E. coli* harboring a *nagA* deletion (BRL04) was graciously provided by Ben Lundgren along with pBRL178, a plasmid encoding the bicistronic expression of *agm1* and *uap1*[70-72]. The BRL04 cells were transformed with pBRL178 and cultured to mid-log phase in a LB medium supplemented with variable amounts of IPTG inducer and either Ac_4GlcNAc or Ac_4GlcNAZ. The cells were then washed and labeled with AlexaFluor 488-Phosphine, and their fluorescence was quantified via flow cytometry (**Figure 2.2)**. It is clear that induction of the salvage pathway had an effect on the azide incorporation into sugars displayed on the outer surface of the *E. coli* (**Figure 2.2).** It was later found that the cells which were apparently labeled in the absence of an azido-sugar where in fact just made permeable to the dye by induction of the salvage pathway. We showed this was case by also labeling permeable cells with propidium iodide. When the permeable cells were removed from the analysis, azide-specific labeling was only observed in cells with both active salvage pathways and Ac_4GlcNAZ supplemented media (**Figure 2.2c,d** and **Figure 2.3**). We also showed that we were able to label approximately 30% of all cells using total cell count, not just the number of non-permeable cells (**Figure 2.3b**).

Discussion

We have shown that *E. coli* containing a *nagA* deletion and heterologously expressing a bicistronic GlcNAc salvage pathway (*agm1* and *uap*1) from *S. cerevisiae* is able to take up and use GlcNAZ in glycans displayed on the outer surface of the bacterium. We saw that the labeling of azido-sugar displaying *E. coli* was dependent on the strength of inducer concentration (**Figure 2.2**) and that a significant fraction of the population was observed to be labeled by flow cytometry (**Figure 2.3**).

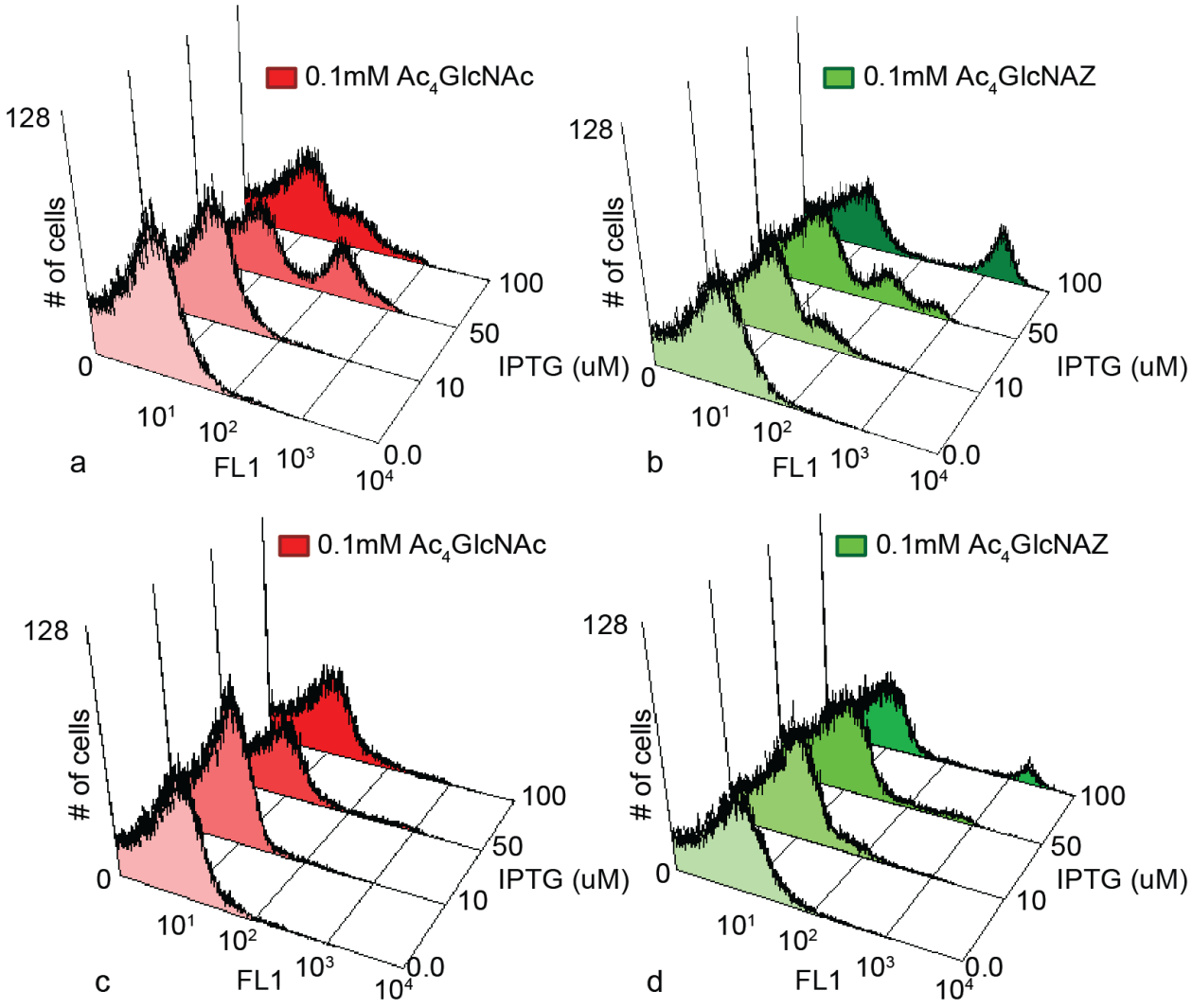

Figure 2.2: Azide-specific labeling via induction of GlcNAZ salvage pathway. BRL04 cells were transformed with pBRL178 and cultured to mid-log phase in a LB medium supplemented with variable amounts of IPTG inducer and either 0.1mM Ac_4GlcNAc or Ac_4GlcNAZ. The cells were labeled with AlexaFluor 488-Phosphine, and their fluorescence was quantified via flow cytometry (FL1, arbitrary units). The permeability of cells was assessed by also incubating them with propidium iodide. Cells assessed as permeable to both dyes were removed from the analysis in the lower panels (**c,d**).

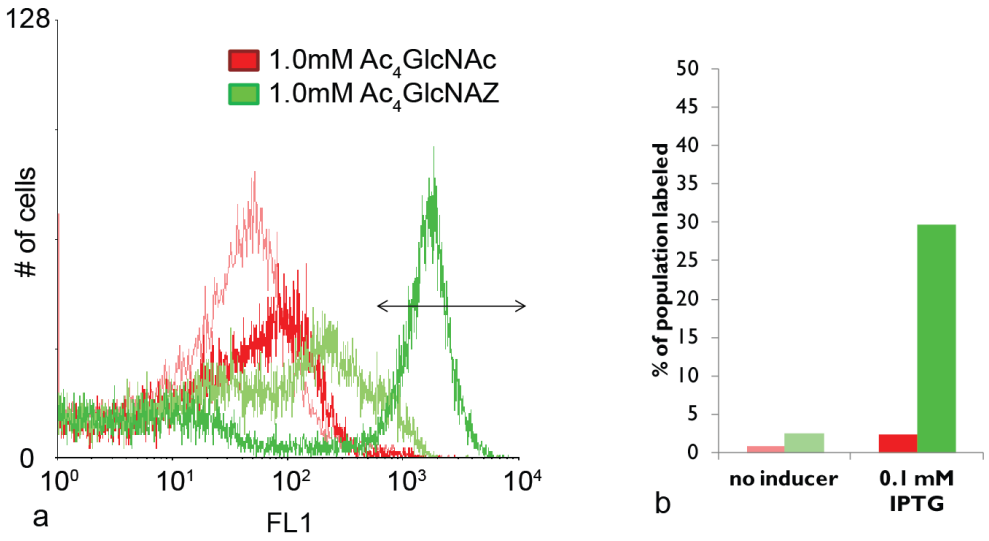

Figure 2.3: Population analysis of azide-labeled *E. coli*. BRL04 cells were transformed with pBRL178 and cultured to mid-log phase in a LB medium supplemented with either no inducer or 0.1mM IPTG and either 1.0mM Ac_4GlcNAc or Ac_4GlcNAZ. The cells were labeled with AlexaFluor 488-Phosphine, assessed for permeability with propidium iodided, and had their fluorescence quantified via flow cytometry. An FL1 signal of 500 to 10,000 was established as "labeled" and the fraction of each population in that range was evaluated. Cells assessed as permeable to both dyes were removed from the analysis.

Immediate future work on this project would include optimizing induction conditions for the expression of the GlcNAc salvage pathway. As we observed, induction of this pathway is required for the azido-sugar to be displayed on the surface of *E. coli*, but it also causes the cell to become permeable to two different fluorophores (**Figure 2.2**). After removing the permeable cells from the data analysis, approximately 30% of the population was labeled. While this labeling percentage is significant, pushing the fraction of azido-sugar displaying cells up to 100% via optimization of induction conditions (i.e. IPTG concentration, culture temperature, and culture medium) is desirable if this method is to be further developed.

Danielle Dube and colleagues have proposed to use azido-sugars in several different drug therapies, including an immunotherapy and an antimicrobial therapy[73, 74]. These applications are viable because of the bioorthogonal and biocompatible nature of the chemistry

used to conjugate drugs to azido-sugar displaying cells. Large-scale production of the azido-sugars necessary for these treatments is an obstacle to overcome in the development of these drugs. Alternatively, we propose the use the use azido-sugars in the formulation of new vaccine candidates. As discussed in several other chapters of this work, Outer Membrane Vesicles (OMVs) are capable of carrying and displaying polysaccharides from the outer membranes of the bacteria from which they originate. Thus, we expect OMVs produced from recombinant *E. coli* that have incorporated GlcNAZ into their endogenous glcyans, specifically the Lipid-A core glycan, will display azido-sugars on their surface which can be used as convenient "handles" for chemical functionalization and conjugation, leading to the formation of a new host of vaccine candidates.

Materials and Methods

Bacterial strains and plasmids. The strains and plasmids used in this chapter are described below (**Table 1.1**) and were generously provided by Benjamin Lundgren. Briefly strains are based on the well-known strain *E. coli* K-12 MG1655. The strain BRL04 was constructed through the use of a λ(DE3) lysogen, Tn5 transposon, and P1 transduction[70]. The plasmid pBRL178 has the CDRs for *agm1* and *uap1* from *S. cerevisiae* expressed bicistronically under control of a T7 promoter[71].

Azido-sugar labeling and flow cytometry. Briefly, BRL04 cells were transformed with pBRL178 using electroporation. Transformed cells were selected on medium supplemented with the appropriate antibiotic. Bacterial cells were labeled using a previously described method optimized for *H. pylori*[69]. An overnight culture of a single colony was selected and grown

overnight in Luria Bertani (LB) medium. Saturated overnights were subcultured 1:50 in LB supplemented with appropriate antibiotics and IPTG as well as a range of Ac_4GlcNAc or Ac_4GlcNAZ (generously provided by Danielle Dube) concentrations. The cultures were grown to mid-log phase ($OD_{600} \approx 0.6$) at which point cells were pelleted via centrifugation at 6,000xg for 10 minutes for, washed once with PBS, and resuspended to $OD_{600} \approx 3.0$ in PBS with 100mM AlexaFluor 488-Phosphine (generously provided by Danielle Dube). Cells were incubated at room temperature for 4 hours before being pelleted and washed three times with PBS to remove unconjugated AlexaFluor 488-Phosphine. Cells were resuspended to a final $OD_{600} \approx 0.1$ before being stained with propidium iodided (Sigma) and assayed for fluorescence via flow cytometry on a FACSCalibur (BD Biosciences).

Table 1.1: Bacterial strains and plasmids used in this chapter.

Strain	Genotype	Source
-BRL04	*λ*(DE3)*nanT*::Tn5(kan)-I-SceI *nanA*::tet Δ*nagA*	[70]
Plasmid	**Description; Resistance marker**	
-pBRL178	IPTG induced T7 biscistronic expression of *S. cerevisiae agm1* and *uap1*; Amp	[72]

CHAPTER 3

PROTEIN GLYCOCONJUGATE OMV VACCINES

Introduction

Bacterial glycans are key components in how bacteria interact with their environments. Polysaccharides present in, on, and around bacterial outer membranes help the cells with colonization of new environments, protection from biological threats, and modulation of host immune response. As complex carbohydrate molecules are integral to the interface between a bacterial cell and its environment, they are often key virulence factors during pathogenesis. Examples of these virulence factors include extracellular polysaccharides which facilitate biofilm formation. Pathogens like enteroaggretive *E. coli* (EAEC) use biofilms to colonize and survive in normally hostile, abioitc environments such as urinary tracts[75]. Capsular polysaccharides are an example of membrane associated polysaccharides that are often associated with pathogenesis. Attachment of the capsular polysaccharide of the Gram- positive pathogen *Streptococcus pneumoniae* to its cell wall is crucial for its pathogenesis of invasive disease[76]. Another example of a capsular polysaccharide virulence factor is the polysialic acid produced by the Gram-negative pathogen *Nesseria meningitidis* type B. The polysialic acid produce in the capsule of *N. meningitidis* B mimics glycans present on host cells, allowing the pathogen to evade the immune response[77]. Though not a polysaccharide, *per se*, the glycans present on N-linked glycoproteins play an apparent role in the colonization of *C. jejuni* as disruption of the *pgl* locus results is decreased infectivity of the pathogen[78]. The roles of polysaccharides and glycans as mediators of pathogenesis are clear, making them attractive targets for vaccine candidates.

In order for a glycan targeted vaccine to be successful, it must be able to generate a robust and long lasting immune response by inducing the formation of glycan specific, class-switched antibodies. A fundamental problem with this approach is that subunit vaccines consisting of bacterial glycans and polysaccharides have generally been unable to elicit this type of immune response. Glycan antigens are generally T-cell independent antigens which means B-cells generating glycans specific antibodies are unlikely to undergo class switching from IgMs to other more potent isotypes and are unlikely to generate any glycan specific memory B-cell or T-cells[39]. This lack of development of B-cells with glycan specific antibodies is due to their inability to recruit cognate T-cells as carbohydrate antigens are generally not loaded onto MHCIIs. A modern method for overcoming this limitation involves chemically conjugating the carbohydrate antigen onto a protein carrier that is known have robust TCR binding epitopes. By endocytosing these glycoprotein conjugates, B-cells with glycan specific antibodies are able to process and display TCR epitopes on MHCII, allowing for clonal expansion and differentiation into plasma cells and memory B-cells [4, 5]. This approach led to the creation of successfull vaccines against *Haemophilus influenzae*, *Streptococcus pneumoniae*, *Nesseria meningitidis*, and others[3, 5].

Though this method of creating protein glycoconjugates via chemical semi-synthesis led to the production of several vaccines, there are several drawbacks associated with it. First, this approach requires the isolation of polysaccharide directly from pathogens which must be cultured to sufficient density. Pathogens can be difficult to culture, often requiring esoteric nutrients in their growth media to reach sufficient density. Adding in safety concerns and the associated costs makes the large-scale culturing of pathogens an unappealing prospect for

making a product that does not have an associated medical urgency. Similarly, the chemistry for protein glycan coupling can be untargeted and inexact, requiring costly purification of the glycoprotein. These concerns can be addressed by protein glycan coupling technology (PGCT), which enzymatically creates glycoproteins using wholly recombinant components [24]. Using PGCT, novel glycoprotein vaccine candidates have been made against several bacterial pathogens[9, 10, 26, 28]. Potential vaccines against one target pathogen in particular, *Francisella tularensis*, have benefited from this technology.

F. tularensis is an intracellular Gram-negative pathogen that is classified as a biodefense category A pathogen by the NIAID due to its high infectivity and ease of dissemination. No licensed vaccine against it currently exists though there is a live vaccine strain (LVS) that can be administered to at-risk populations[79]. Like most Gram-negative pathogens, *F. tularensis* has an outer membrane comprised primarily of lipopolysaccharide (LPS). The major antigenic subunit of this LPS is a repeating oligosaccharide subunit known as an O-antigen. In previous studies examining the immune response against *F. tularensis* and the effectiveness of potential vaccines, it has been shown that an immune response against the O-antigen is helpful for clearing infection[80-82]. In an attempt to create a more effective vaccine, PGCT in *E. coli* was used to create a protein glycoconjugate vaccine against *F. tularensis* using a recombinant O-antigen biosynthetic pathway, *C. jejuni* PglB as the OST, and a detoxified *Pseudomonas aeruginosa* exotoxin A as the carrier protein[83]. This purified glycoconjugate vaccine was able to generate a robust humoral immune response against the O-antigen and confer an extended time to death on mice infected with *F. tularensis holoartica*, one of the less virulent strains of *F. tularensis*. More recently, the DeLisa Research Group has produced a glycOMV vaccine that was

able to confer protection against lethal challenge with the highly virulent *F. tularensis* ShuS4 strain in mice[16]. These works suggest that a possible direction for future vaccines.

In this chapter, I will discuss combining the two previous approaches using PGCT and OMVs to create a single vaccine formulation. My approach uses the versatility and specificity of PGCT and combines it with the immunostimulatory power of OMVs. It can be generalized to any Gram-negative pathogen possessing an O-antigen, but as a first target, I have chosen *F. tularensis*. By expressing the recombinant O-antigen pathway from *F. tularensis* in an appropriate glycoengineered hypervesiculating strain of *E. coli* along with an appropriate periplasmically expressed carrier, I have created OMVs containing lumenal glycoprotein antigens. The carrier protein chosen for this study were scFv13R4-4xGT, a single chain variable fragment whose soluble expression in the periplasm of *E. coli* has been optimized and conjugated to a "4xglyc-tag", MBP-4xGT, *E. coli* maltose-binding protein conjugated to a "4xglyc-tag" which has been shown to have strong TCR binding epitopes[84], and EPA, *Pseudomonas aeruginosa* exotoxin A which has been genetically modified to no longer be toxic and has two bacterial glycosylation sites engineered into sequence[10]. Conjugating the *F. tularensis* O-antigen to these carrier proteins and loading them into an OMV is expected to elicit a more robust and long term immune response to the O-antigen and thus provide better protection against *F. tularensis* challenge than either the glycoconjugate or glcyOMV alone. Additionally, we have performed *in vitro* protein glycosylation (IVPG) on OMVs displaying ClyA-GT, *E. coli* hemolysin A conjugated to a "4xglyc-tag".

Results

Selection of an appropriate glycoengineered, hypervesiculating strain for *in vivo* PGCT. To produce OMVs containing a higher yield of glycoproteins, we tested several hypervesiculating strains for their ability to produce glycoconjugates both in the periplasm and in OMVs. The well-studied hypervesiculating strain JC8031 that contains knockouts of *tolR* and *tolA* was used as a starting point for the production of glycoproteins [85]. However, it is known that by knocking out the endogenous *waaL* gene, the transfer of glycans from UPP to Lipid A is abolished, leading to an increase in the LLO substrate available to PglB. This increase in the substrate pool is thought to increase the glycosylation efficiency for the PGCT. The DeLisa Research Group previously took advantage of this by creating the strain JC8032, which is JC8031Δ*waaL[24]*. Alternatively, the strain CLM24 has been shown by our lab and others to be able to produce efficiently glycosylated proteins [9, 10, 24, 86]. In order to increase the yield of OMVs from CLM24, we took advantage of the previous observation that knocking out *nlpI* from *E. coli* yields a hypervesiculating strain with no significant detriment to cell viability or membrane integrity [50]. By comparing production of carrier proteins to glycosylated carrier proteins in the periplasm of these three strains, we can see that CLM24Δ*nlpI* produces the most glycoconjugate (**Figure 1.1**). The characteristic O-antigen MW laddering that is a result of variable polymer length is clear in all cases where active PglB was expressed. Most the glycoprotein appears at or slightly above the MW for aglycosylated MBP-4xGT (**Figure 1.1 bottom**). This intense band around the MW for MBP-4xGT suggests that the glycosylated form predominantly contains lower order oligomers of O-antigen subunits.

By also comparing the amount of glycoproteins in OMVs produced from these strains, we again see that CLM24Δ*nlpI* produces OMVs containing the most glycoprotein (**Figure 3.2**) relative to total protein content. While the trend observed here is using maltose-binding protein as the carrier, a similar trend was observed for both scFv13R4 and *Pseudomonas aeruginosa* exotoxin A (EPA) (**Figure 3.3**) (Data not shown for production of scFv13R4 and EPA in JC8031 or JC8032). In creating CLM24Δ*nlpI*, we have constructed a hypervesiculating strain of *E. coli* well suited for performing *in vivo* glycosylation

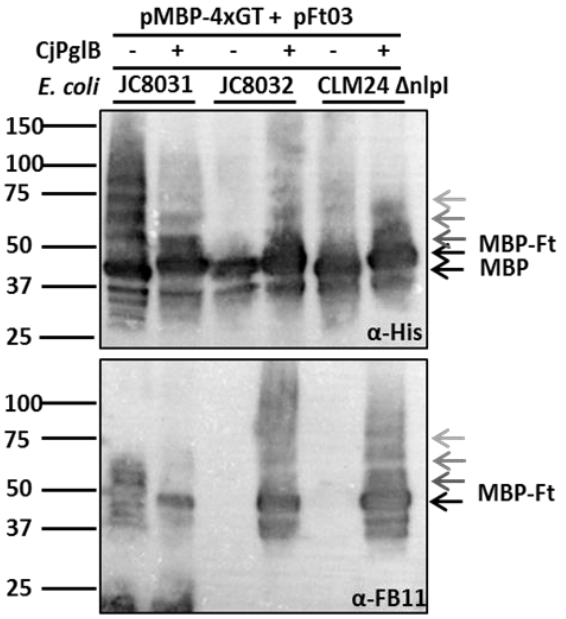

Figure 3.1: Comparison of periplasmic glycoprotein yield in three hypervesiculators. The protein MBP-4xGT was targeted for periplasmic expression in strains expressing the biosynthetic pathway for *F. tularensis* O-antigen. The glycoprotein yield was compared using Western blotting. Top is the anti-His blot for MBP detection and bottom is the anti-Fb11 blot which detects the *F. tularensis* O-antigen. The (-/+) represents the inactive (-) vs. active (+) *C. jejuni* PglB. All samples were normalized by total protein content as determined by BCA. Note: This Western blot was performed by Dr. Kristina Overkamp.

The glycosylation pattern of scFv13R4-4xGt and EPA shows that they are present in OMVs and that they are protected from degradation with proteinase K (**Figure 3.3**). This observation suggests that EPA is located within the OMVs and that the proteinase cannot

access it for degradation. The evidence for lumenal glycoproteins is strengthened by the observation that lysing the OMVs prior to proteinase treatment by boiling them removes the signal from EPA and that glycoforms are only present in OMVs produced from cells expressing active PglB (**Figures 3.2 and 3.3**). The prominent lower molecular weight bands apparent in the EPA OMVs are likely EPA degradation products (**Figure 3.3 bottom right**). As the two engineered glycosylation sites on EPA are internal, it is probable that EPA is getting cleaved at a site between them, resulting in two lower molecular weight bands whose mass sum to that of full-length EPA. Additionally, we have often observed a strong 50kDa band in the anti-His blot for EPA, suggesting that this larger fragment is the C-terminal fragment containing the His tag. Indeed, EPA is known to have a protease specific site that is key to its biological function between the N- and C-terminal domains[87].

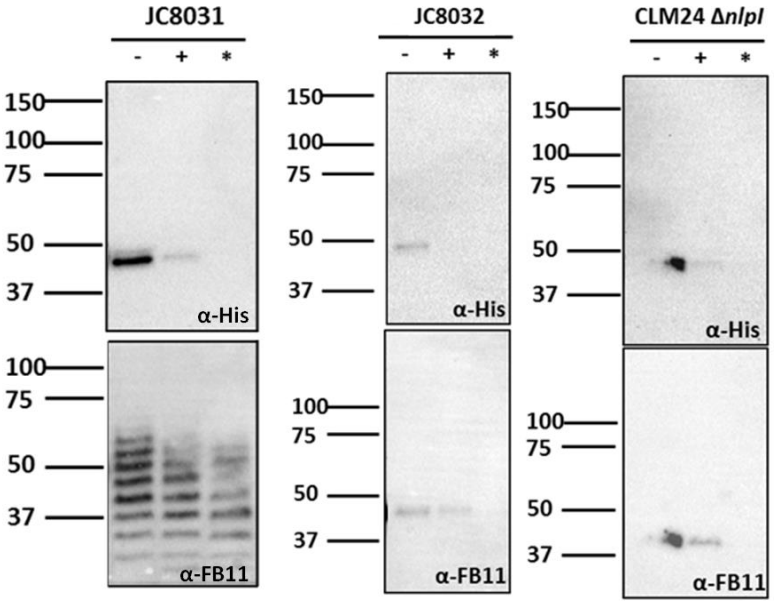

Figure 3.2: Comparison of glycoproteins in OMVs from three hypervesiculators. The protein MBP-4xGT was targeted for periplasmic expression and subsequent glycosylation and loading in the lumen of OMVs. Top is the anti-His blot for MBP detection and bottom is the anti-Fb11 blot which detects the *F. tularensis* O-antigen. The OMVs were either left untreated (-), were treated with proteinase K (+), or pre-boiled before being treated with proteinase K (*). The proteinase K digestion shows that glycoprotein antigens are indeed loaded in vesicles and partially protected from degradation with proteinase K. Samples were normalized by total protein content as measured by BCA. Note: These Western blots were performed by Dr. Kristina Overkamp.

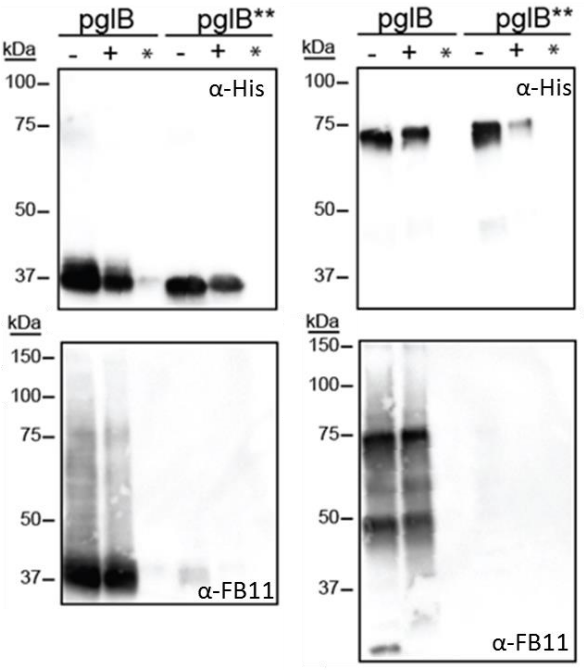

Figure 3.3: Use of Clm24Δ*nlpI* to produce glycoprotein loaded OMVs. The carrier proteins used here are scFv13R4-4xGT and EPA. They have been targeted to the periplasm for glycosylation with *F. tularensis* O-antigen and subsequent loading into OMVs. Top is the anti-His blot for carrier protein detection and bottom is the anti-Fb11 blot which detects the *F. tularensis* O-antigen. The cells were expressing *C. jejuni* PglB in either wild-type PglB (pglB) or catalytically inactive double mutant PglBD54NE316E (pglB**). The OMVs were either left untreated (-), were treated with proteinase K (+), or pre-boiled before being treated with proteinase K (*). The proteinase K digestion patterns show that glycoprotein antigens are indeed loaded in vesicles and protected from degradation with proteinase K. Samples were normalized by total protein content as measured by BCA.

Determining optimal conditions for *in vitro* protein glycosylation (IVPG) using recombinant *F. tularensis* O-antigen LLOs. As a proof of concept to demonstrate LLOs containing immunologically relevant recombinant oligosaccharides can be used as a substrate for *in vitro* glycosylation, we have performed IVPG on both MBP-4xGT and EPA using purified carrier proteins, purified LLO extracts from *E. coli* CLM24 transformed with the plasmid encoding the biosynthetic pathway for *F. tularensis* O-antigen to produce *E. coli*/*F.tularensis* hybrid LLOs, and purified *C. jejuni* PglB. After several attempts, we found that running the IVPG reaction at 30˚C for 6 hours resulted in the most efficient protein glycosylation as determined by densitometry of Western blots comparing intensities of glycosylated vs. a-glycosylated bands (data not

shown). During these optimization experiments, it was determined that the detergent DDM in the IVPG reaction buffer caused oligomerization of EPA, but adding the rest of the IVPG reaction components resolved the oligomer back into a monomer on Western blots (**Figure 3.4 top**). We have shown that is possible to glycosylate EPA and MBP-4xGT using IVPG (**Figure 3.4**) and that while overall glycosylation efficiency may be lower, the transfer of higher order O-antigen polymers is much greater when using IVPG as compared to the glycoproteins produced *in vivo* **(Figure 3.4 bottom)**.

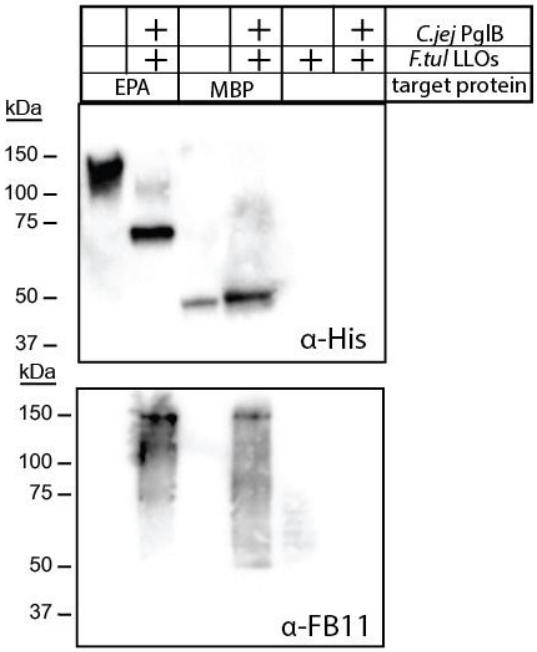

Figure 3.4: *In vitro* glycosylation of MBP-4xGT and EPA with O-antigen. Figures above show anti-His (top) and anti-FB11 (bottom) Western blots of *in vitro* protein glycosylation reactions performed at 30^{o}C for 6 hours. Samples were normalized by purified protein content (10µg) as measured by BCA. The (+) indicates the presence of the associated reaction component. The right two lanes are negative controls

***In vitro* protein glycosylation can be used to directly glycosylate outer membrane proteins displayed on OMVs.** To develop a novel method for creating glycoprotein containing OMVs, we have performed IVPG directly on proteins displayed by OMVs. Here, we have the previously generated *E. coli* hemolysin construct with a 4xGlycTag and expressed in the hypervesiculating strain JC8031[85]. We then took those OMVs and used them as substrates for IVPG. Not

knowing whether these OMVs could function as suitable substrates for the *in vitro* reaction, we performed IVPG using *C. jejuni* PglB and its native heptasaccharide substrate as well as the *F. tularensis* O-antigen LLOs. Upon subsequent Western blotting, we saw the apparent formation of glycosylated ClyA-4xGlycTag when both LLOs were used as substrates (Data not shown). After establishing that ClyA-4xGlycTag can be glycosylated in OMVs, we then showed through density gradient ultracentrifugation that the OMVs remained intact after undergoing *in vitro* glycosylation (**Figure 3.5**).

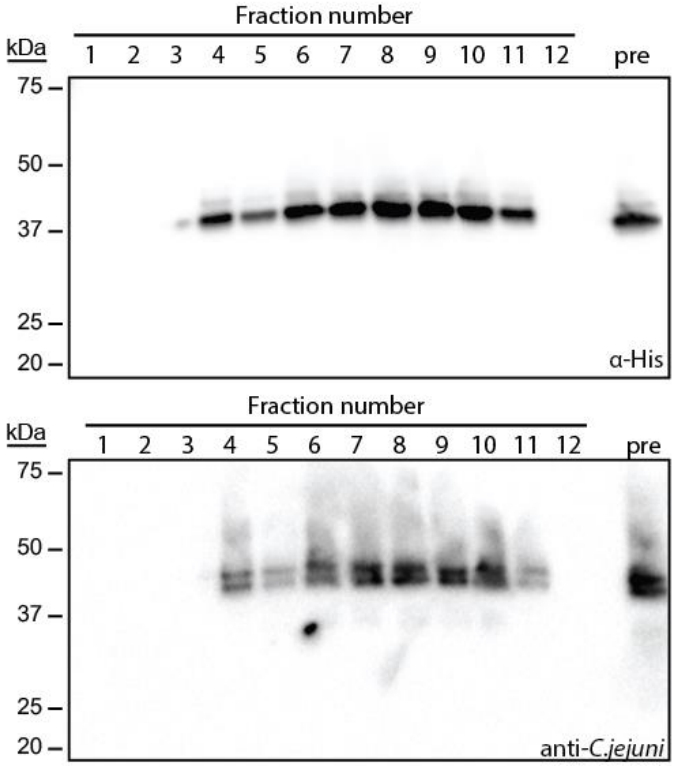

Figure 3.5: Density gradient fractionation of OMVs glycosylated *in vitro*. The *E. coli* hemolysin A (*clyA*) was modified to have a 4x-GlycTag at its C-terminus. OMVs ClyA-4xGlycTag were used as substrates for IVPG with purified *C. jejuni* PglB and recombinant heptasaccharide LLOs. Those OMVs were then subjected to density gradient ultracentrifugation and subsequent Western blotting for detection of the protein with an anti-His antibody and detection of glycoprotein with anti-*C. jejuni* glycan antibody. Lanes are numbered by fractions with increasing density (1 being lowest and 12 being highest). The lane labeled "pre" shows the whole OMV prep before it is subjected to density gradient ultracentrifugation.

Discussion

We have created a glycoengineered, hypervesiculating strain of *E. coli* as a platform for the production of glycoconjugate OMV vaccines (CLM24Δ*nlpI)*. We have shown production of three different *N*-linked glycoproteins with the *F. tularensis* O-antigen in CLM24Δ*nlpI* and that all three glycoproteins are protected from proteinase K degradation, which is consistent with the expected lumenal packaging of these glycoprotein antigens. As most of the glycoproteins we observed in OMVs had low order oligomerization of the O-antigen subunits, it may be that cargo protein size is a limiting factor in packaging lumenal OMV proteins. It may be that glycoconjugates with higher order oligomers are essential to eliciting a protective immune response. If this were to be the case, or second method for producing glycoconjugate OMV vaccines would be able to overcome it.

The toxin hemolysin A (ClyA) has been used as a carrier protein to shuttle recombinant protein antigens to the surface of recombinant OMVs[13, 14, 24, 88]. It has also been modified with a 4xGlycTag and used as a substrate for *in vivo* protein glycosylation by *C. jejuni pgl* pathway. Using *in vitro* protein glycosylation, we have shown direct glycosylation of ClyA-4xGlycTag with both the *C. jejuni* heptasaccharide and the *F. tularensis* O-antigen. As expected from our previous *in vitro* glycosylation reactions with the *F. tularensis* O-antigen, the favored glycoprotein product consisted of longer length repeating O-antigen subunits. Additionally, we showed that the OMVs remained as intact liposomes after undergoing *in vitro* glycosylation by subjecting them density gradient ultracentrifugation and subsequent Western blotting. We clearly observed the co-localization of glycosylated ClyA in the same density regions where OMVs settle during ultracentrifugation. Using this direct *in vitro* glycosylation reaction on OMVs

may make it possible to create glycoprotein OMV vaccines that are intractable for *in vivo* glycosylation reactions.

The next step in this research is to evaluate the effectiveness of these glycoconjugate OMVs in an animal model. Performing a series of immunizations and challenges similar to those done by Chen, et al against *F. tularensis* would allow us to directly compare the effectiveness of this vaccine against glycOMVs. Future studies should include the *lpxM* deletion in ClM24Δ*nlpI* as this would allow for the creation of less reactogenic OMVs[16, 89]. It may also be that there are PglB homologs that are more efficient at transferring the *F. tularensis* O-antigen that should be used instead of the *C. jejuni* OST[90, 91]. We would directly compare the mouse immune response to O-antigen glycosylated lumenal EPA and glycosylated outer membrane displayed ClyA to each other as well as the purified glycoproteins by themselves. Unlike the *F. tularensis* glycolipid alone, we would expect there to be some immune response to the glycoprotein antigens alone. This comparison would allow to evaluate the immunostimulatory effects of OMVs on the glycan specific immune response to protein glycoconjugates. If these formulations of glycoprotein containing OMVs are not protective, we propose the use *F. tularensis* protein carriers that are known to have strong TCR binding epitopes[92].

As previously discussed, the mechanism by which glycOMVs generate such a strong and protective antibody response remains elusive. A direct comparison of glycOMVs with more traditional glycoconjugate proteins loaded into OMVs may provide some insight into the immune response to glycolipids presented on OMVs. The use of multiple glycoprotein antigens (MBP, EPA, and ClyA) presented to the immune system in different contexts (lumenal vs. displayed) may also shed some light on the adaptive immune response to OMVs. Indeed it may

be that specific formats of glycoprotein containing OMVs can be tailored to specific pathogens of interest. If the immunization and challenge studies are carried out over longer time periods, we may find that glycoprotein containing OMVs provide a stronger, more protective immune response over longer time scales. In addition, if the immune response to glycoproteins with bacterial oligosaccharides is robust it may be that we could use engineered human-like glycans to create immunotherapies[15, 25].

Materials and Methods

Bacterial strains and plasmids. The strains and plasmids used in this chapter are described below (**Table3.1**). Briefly strains are based on the well-known hypervesiculating strain JC8031 whose phenotype is attributed a knockout of *tolRA*, and CLM24, strain which lacks the *waaL* ligase[9]. Plasmid features are outlined below.

Creation of hypervesiculating knockout strain via P1 transduction. Briefly, donor phages were created by incubating P1 phage with the member of the Keio collection that contains the *nlpI* gene knockout replaced by kanamycin [93]. After complete lysis of the donor culture, phage sample was clarified via centrifugation and stored at 4˚C until used. These phages were incubated with the CLM24 and incubated for 30 minutes at 37˚C. Lysis of the recipient phage was halted via the addition of 1mM sodium citrate before the cells were plated on kanamycin and sodium citrate. Several colonies were restreaked on kanamycin and sodium citrate. Knockout was verified by observation of hypervesiculation.

Cell growth and subcellular fractionation of glycoproteins. Briefly, plasmids containing the necessary genes for *N*-linked protein glycosylation (**Table 2.1**) were transformed into different

strains using electroporation. In total, three plasmids are generally required for protein glycosylation: a periplasmically expressed target protein, a biosynthetic pathway for LLO, and an OST. Transformed cells were selected on medium supplemented with the appropriate antibiotic. An overnight culture of a single colony was selected and grown overnight in Luria Bertani (LB) medium. Saturated overnights were subcultured 1:50 in LB supplemented with appropriate antibiotics. The cultures were grown to mid-log phase ($OD_{600} \approx 0.6$) at which point, target protein and PglB were was induced with an appropriate combination of L-arabinose (0.2%) and IPTG (0.1 mM). Induction was allowed to proceed for 16-20 hours at 37˚C. Cells were pelleted via centrifugation at 6,000xg for 10 minutes for subsequent subcellular fractionation. Whole cell fractions were simply removed and stored at -20˚C until they were used. Periplasmic fractions were obtained via previously described methods[94]. Briefly, pelleted cells were incubated on ice for 30 minutes in a buffer with high osmolarity (2M sucrose) and 0.15mg/mL lysozyme. Cells were then spheroplasted by osmotic shock via rapid dilution of the high osmolarity buffer. Spheroplasts were pelleted via centrifugation at 6,000xg for 10 minutes, and the periplasmic fraction was decanted from the supernatant. The OMV fractions were prepared as previously described[88]. Cell-free culture supernatants were collected post induction and filtered through a 0.2 μm filter. Vesicles were isolated by ultracentrifugation (Beckman-Coulter; TiSW28 rotor; 141,000xg; 3 h; 4˚C) and resuspended in PBS. OMVs were quantified by the bicinchoninic-acid total protein assay (BCA Protein Assay; Pierce) using BSA as the protein standard.

Purification of target proteins for glycosylation. The purified MBP and EPA to be used as target protein for *in vitro* glycosylation were purified from the periplasm via previously established

methods[94]. The periplasmic extract of cells was loaded onto charged Ni-NTA resin in a gravity column in 10mM imidazole. The resin was then washed with 30mM imidazole before the target proteins were eluted with 200mM imidazole. Proteins were then concentrated to >1mg/mL via diafiltration 5kDa MWCO centrifugal filtration units (Millipore) into PBS (pH=7.0).

Purification of PglB and LLOs. Purification of PglB and LLOs was carried out as previously described with a few modifications[91]. Briefly, CLM24 cells were transformed with pLAFR-F.tularensis, pACYC-*pgl::pglB*, or psN28-pglB[12]. Cells were subcultured to mid-log phase and induced with 0.2% L-arabinose where appropriate. After an 18 hour induction, cells were pelleted by centrifugation at 10,000 x g for 15 min. Pellets were resuspended in 50mM TrisHCl and 25mM NaCl (pH=7.0) at a concentration of 10mL per gram of pellet. Cells were lysed by freeze thaw, treated with 0.1µg/mL DNase, and homogenized using a microfluidizer. Lysate was clarified by centrifugation at 15,000 x g for 20 min. Membrane extract was pelleted from supernatant by ultracentrifugation at 141,000 x g for 1 hour. Extracts were re-suspended using a manual homogenizer in 50mM TrisHCl, 25mM NaCl, and 0.1% N-dodecyl β-D-maltoside DDM(pH=7.0) to a final volume of 1 mL per gram of initial cell pellet. All buffers from this point on were modifications of this base recipe. Extracts were clarified by centrifugation at 16,000 x g for 1 hour, and supernatant was stored at 4^{o}C. For PglB purification, the solubilized membranes were supplemented with 10 mM imidazole and incubated with Ni-NTA resin for 1 hours at room temperature. The PglB loaded resin was then applied to a gravity flow column and washed with 60 mM imidazole before PglB was eluted with 200 mM imidazole. The purified protein was then injected onto a Superdex 200 gel filtration column using AKTA-FPLC (GE Healthcare, Waukesha, WI) and fraction containing PglB were collected and assayed for activity.

Plasmids carrying glycan biosynthesis pathways were freshly transformed into CLM24 cells which were subsequently cultured LB. The culture was allowed to grow at 37˚C until OD_{600} ≈ 0.8 where the temperature was shifted to 30˚C and the culture was allowed to express O-antigen biosynthesis pathway for 16 hours. The next day, cells were harvested and completely dried in a lyophilizer. The dried cell pellet was incubated with 10:20:3 v/v/v chloroform/methanol/water for 30 min. The organic layer was kept and the solvent was removed, yielding a dried extracted LLOs, which was then resuspended in glycosylation buffer.

***In vitro* glycosylation reactions.** The *in vitro* glycosylation reaction was carried out as previously described [12]. Briefly, target proteins EPA at 20μg/mL, MBP at 10μg/mL, and ClyA OMVs at 10μg/mL were added to purified PglB or PglB** at 30μg/mL and *F. tularensis* or *C. jejuni* LLOs at 100μg/mL in 10mM HEPES, 11mM $McCl_2$, and 0.1%N-dodecyl β-D-maltoside (DDM) (pH=7.4). Reactions were allowed to run for 6 hours at 30^{o}C.

Density gradient ultracentrifugation. To ensure that the glycans detected on OMVs after *in vitro* glycosylation are OMV associated and that those OMVs are intact liposomes, glycosylation OMV samples were further purified by density gradient ultracentrifugation as previously described [88]. Briefly, OMVs were suspended in HEPES buffer (pH=6.8) instead of PBS and diluted into Optiprep solution to a final concentration of 1.0mg/mL in 1.5mL of 45% Optiprep solution in HEPES. Discrete layers of Optiprep/HEPES were added to a 12mL ultracentrifuge tube by carefully pipetting more dense layers below less dense layers. Each layer was added in 330μL fractions with the following % composed of Optiprep: 10%, 15%, 20%, 25%, 30%, 35%, 1.5mL OMV fraction containing 45% Optiprep, 9.0mL of 60% Optiprep to fill the tube. The gradients were spun at 180,000xg for 3 hours after which thirteen 0.5mL fractions were taken

from the top of the centrifuge tube. The samples were subjected to SDS-PAGE and analyzed by Western blot for the presence of glycosylated ClyA.

Proteinase K degradation assay. To show that lumenal glycoproteins are in fact within the OMVs, recovered OMVs were diluted into PBS to a concentration 100μg/mL and incubated at 37^{o}C for 1 hour either with or without 1mg/mL proteinase K, or were boiled in 1% w/v SDS prior to treatment with 25μg/mL proteinase K to disrupt the OMVs. The digestion reaction was halted via the addition of 1mM phenylmethylsulfonyl fluoride (PMSF), and all samples were boiled prior analysis via Western blotting.

Western blot analysis. Whole cell, periplasmic, and OMV samples were prepared for SDS-PAGE analysis by boiling for 15 min and cooling to room temperature in the presence of loading buffer containing β-mercaptoethanol. Samples were run on 10% cross-linked polyacrylamide gels (BioRad, MiniPROTEAN® TGX) and transferred to a PVDF membrane via semidry transfer. After blocking with a 5% milk in Tris-buffered saline (TBS), membranes were probed with HRP-conjugated anti-His (Abcam) for the detection of carrier proteins (MBP, ClyA, scFv13R4, EPA). When analyzing samples for the presence of *F. tularensis* O-antigen, membranes were first probed with mouse monoclonal Fb11 (Abcam) and visualized with anti-mouse HRP-conjugated secondary (Promega). When analyzing samples for the presence of the *C. jejuni* heptasaccharide, membranes were first probed with the rabbit polyclonal serum HR6P (Aebi lab) before being probed with anti-rabbit secondary (Promega). Signal was visualized using HRP substrate Clarity ECL (BioRad) and imaged with a ChemiDoc XRS+ Imaging System (BioRad).

Table 3.1: Bacterial strains and plasmids used in this chapter.

Strain	Genotype	Source
-JC8031	*supE hsdS met gal lacY tonA ΔtolRA*	[85]
-JC8032	JC8031*ΔwaaL*	[24]
-CLM24	W3110Δ*waaL*	[9]
-CLM24Δ*nlpI*	CLM24Δ*nlpI*; Kan	This study
Plasmid	Description; Resistance marker	
-pGAB2	*F. tularensis* O-PS antigen gene cluster in pLAFR1; Tc	[83]
-pTrc99a	IPTG inducible expression vector; Amp	Lab stock
-pGVXN-150-EPA	arabinose inducible, periplasmic EPA expression vector; Amp	[10]
-pTrc99a-ssDsbA-MBP-4xGlycTag	IPTG inducible expression vector for periplasmic expression of MBP-4xGlycTag; Amp	[24]
-pTrc99a-ssDsbA-scFv13R4-4xGlycTag	IPTG inducible expression vector for periplasmic expression of MBP-4xGlycTag; Amp	[95]
-pBad18a-ClyA-4xGlycTag	Arabinose inducible expression vector for ClyA with a GlycTag.	[95]
-pACYC-*pgl*	low copy number plasmid containing *C. jejuni pgl* operon; Chl	[8]
-pACYC-*pgl::pglB*	low copy number plasmid containing *C. jejuni pgl* operon with a knockout of *pglB*; Chl	[8]
-pMAF10-PglB	arabinose inducible expression vector for *C. jejuni* PglB; Tmp	[10]
-pMAF10-PglB**	arabinose inducible expression vector for the catalytically inactive *C. jejuni* $PglB^{D54NE316Q}$; Tmp	[96]
-pSN28-PglB	IPTG inducible expression vector PglB purification; Spec	[12]

CHAPTER 4

POLY-N-ACETYLGLUCOSAMINE DECORATED OMVS AS VACCINES

Introduction

Poly-β-1,6-*N*-acetylglucosamine (PNAG) is a linear polysaccharide that is present on the surface of a wide range of human microbial pathogens [97]. In bacteria, it plays an important role in biofilm formation and host colonization [98-102]. The production of PNAG in bacteria is fairly well understood as there are homologous gene clusters responsible for its biosynthesis. The gene clusters, usually referred to as intercellular clusters of adhesion (*ica* in *Pseudomonas aeruginosa* and *Staphylococcus aureus*) or PNAG synthesis clusters *(pga* in *E. coli*), contain four genes which in *E. coli* are named *pgaA,B,C,D*. [98-100]. The genes *pgaC* and *pgaD* code for proteins associated with the inner membrane and use UDP-GlcNAc as a substrate to synthesize PNAG in the periplasm. Subsequently, *pgaA* and *pgaB* are associated with the outer membrane in Gram-negative bacteria or the outer face of the cytoplasmic membrane in Gram-positive bacteria and facilitate PNAG secretion and de-acetylation, respectively.

PNAG has been used in a variety of immunization and challenge models with varying degrees of success [97, 103-108]. It has been shown that antibodies capable of binding to both acetylated and de-acetylated forms of PNAG can be used to passively immunize animals against pathogens displaying PNAG [97, 107]. Additionally, it has been shown that the de-acetylated form of PNAG is the crucial antigen for generating a protective immune response. In this chapter, I will present a different path to formulating PNAG in a vaccination trial by presenting it on OMVs. Production of the polysaccharide PNAG was facilitated in hypervesiculating strains

of *E. coli* through overexpression of the genes in the PNAG biosynthetic pathway. In order to enrich the PNAG on our OMVs with the acetylated form, we also heterologously expressed the *S. aureus* PNAG deacetylase *icaB* in cells producing PNAG OMVs[109].

Mice were used as model organisms to evaluate the immunological response to PNAG on OMVs as a protective antigen. After immunization of mice, the humoral immune responses to the PNAG OMVs was analyzed by quantifying the present of PNAG specific antibodies in the mice sera. Immunized mice were then challenged I.V. with 10xmLD$_{50}$ of *S. aureus*, and it was observed that PNAG OMVs provided partial protection. Lastly, to demonstrate that the humoral immune response to PNAG OMVs might be protective against a wider range of pathogens, we performed *in vitro* serum bactericidal assays against *F. tularensis* LVS.

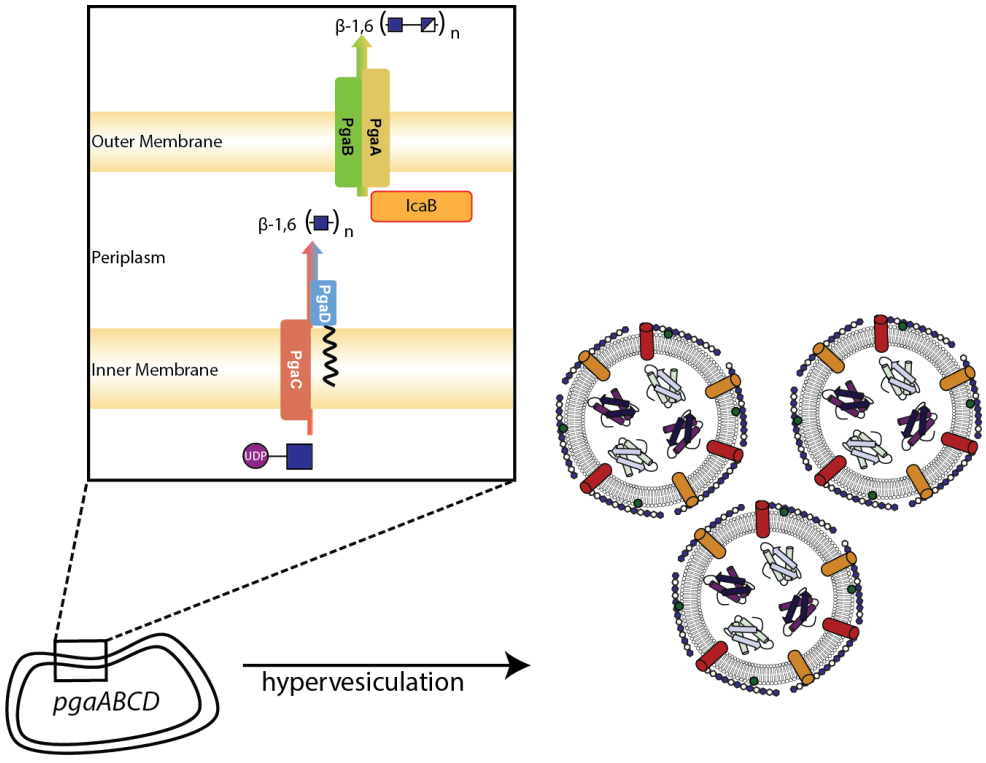

Figure 4.1: Production of PNAG OMVs. Through overexpression of the *pgaABCD* in a hypervesiculating strain of *E. coli*, we will produce PNAG decorated OMVs. By also expressing the *S. aureus* deacetylase IcaB in the periplasm of these cells, we will create PNAG OMVs with a shift of the PNAG polymer toward the deacetylated form. We will also take advantage of the recombinant *E. coli* platform by producing OMVs from a strain with penta-acylated lipid A, greatly reducing the reactogenicity of the OMVs.

Results

Production of PNAG can be augmented in *E. coli*. We first demonstrate that production of PNAG could be enhanced via addition of exogenous copies of the *pga* operon and that the produced PNAG is associated with OMVs. For production of OMVs, we use the *E. coli* strain JC8031, a hypervesiculating strain that contains knockouts of *tolR* and *tolA* [85]. For augmented production of PNAG, the IPTG inducible plasmid pUc18TcP-*pgaABCD* (p*pgaABCD*) containing the PNAG biosynthetic operon from *E. coli* K1 was graciously provided by Gerald Pier. OMVs were harvested from the strain with induced p*pgaABCD* and Western blot analysis showed there was a corresponding increase of PNAG on OMVs (**Figure 4.2a**). We also observed the variable degree of polymerization of PNAG, with polymers ranging from approximately 37kDa to 150kDa (**Figure 4.2a**). These molecular weights correspond to roughly 100 to 500 GlcNAc repeats. We further created the strain JC8031Δ*pgaC* containing an additional knockout of *pgaC*, the first gene in the biosynthetic pathway for PNAG. This strain serves as a negative control for endogenous PNAG production. The knockout was transduced into JC8031 through P1 phage from the corresponding strain in the Keio collection [93]. The relative abundance of PNAG in OMVs produced by the knockout, wild-type, and augmented strains was compared via PNAG specific dot blotting (**Figure 4.2b**). It can be seen from the intensities that knocking out *pgaC* had no effect on the dot intensity, indicating that there is some nonspecific binding (**Figure 4.2b first lane**). Treatment of the OMVs with Dispersin B, a very specific hydrolase that degrades the β-1-6 glycosidic bond in PNAG, showed a reduction in dot intensity to background, indicating that the PNAG being detected is authentic and that it is localized to the outer surface of OMVs

(**Figure 4.2c**). If the PNAG was lumenal, we would expect to see little to no degradation by Dispersin B.

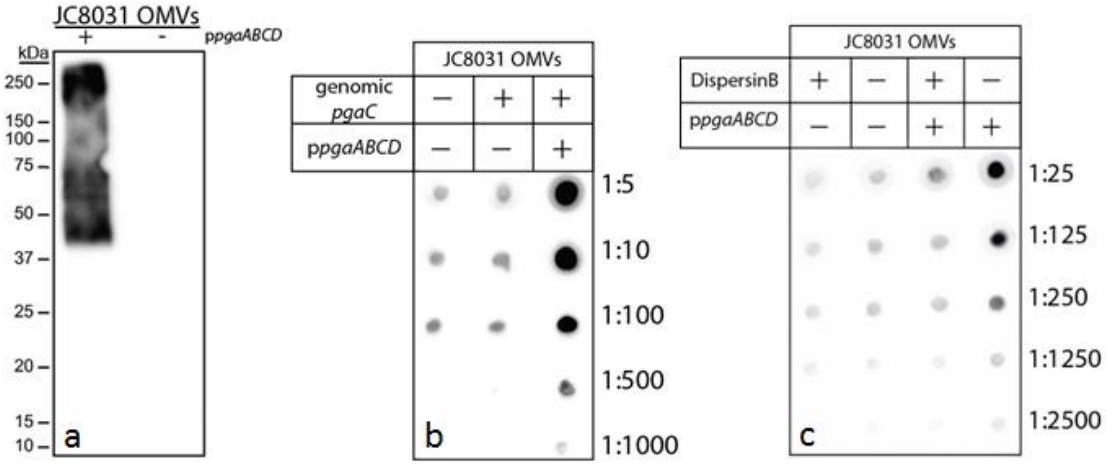

Figure 4.2: Characterization of PNAG on OMVs. OMVs from strains (JC8031 ±Δ*pgaC* ±p*pgaABCD*) were subjected to SDS-PAGE and Western blotting (**a**) or diluted in PBS according to shown dilution scheme (1:1 is 2mg/mL) and spotted on nitrocellulose membranes (**b,c**). The middle panel (**b**) shows relative signal from F598 PNAG binding antibody between negative control, wild type, and overexpressed PNAG pathways. In the right panel (**c**), OMVs were treated with Dispersin B before being dot blotted, reducing the signal from PNAG specific binding.

PNAG is present on the exterior of OMVs. TEM imaging of uranyl acetate stained OMVs produced from JC8031Δ*pgaC*, JC8031, and JC8031 + p*pgaABCD* showed that the overall size and morphology of OMVs was unchanged by the presence of PNAG. There is an interesting observation of a biofilm-like material in OMVs produced from JC8031 + p*pgaABCD* that is likely the result of gelling properties of PNAG at higher concentrations (**Figure4.3c**). To visualize the PNAG directly on the surface of OMVs, we performed immunostaining on OMVs produced from JC8031Δ*pgaC* and JC8031 + p*pgaABCD* using the human monoclonal F598 and gold particle conjugated anti-human secondary (**Figure4.3d**). We were unable to visualize both the membrane and gold particles simultaneously, so OMVs only appear as a faint shadow on the transmission electron microgram. Cluster of the gold conjugated antibodies were observed in

circular patterns consistent with the diameters of OMVs in JC8031 + p*pgaABCD* samples. We did not observe similar trends in the JC8031Δ*nlpI* samples (Data not shown).

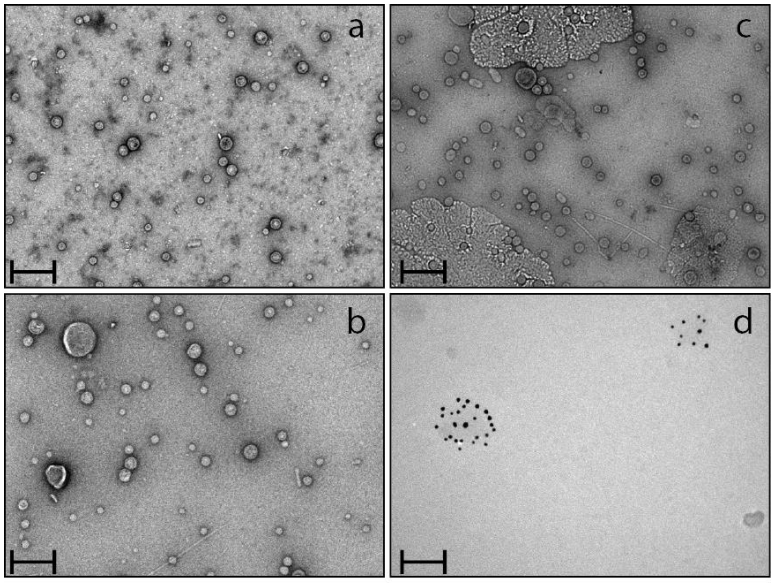

Figure 4.3: TEM of PNAG OMVs. OMVs produced by JC8031Δ*pgaC* (**a**), JC8031 (**b**), or JC8031 +p*pgaABCD* (**c**,**d**) were visualized by TEM. The lipid bilayers of OMVs were observed via staining with uranyl acetate (**a**-**c**). Some islands of biofilm formation can also be seen when p*pgaABCD* is overexpressed (**c**). PNAG OMVs were also subjected to immunostaining with F598 and subsequent visualization with gold-conjugated anti-human secondary (**d**). The total protein concentration of OMVs used in **a-c** is 100µg/mL while 10µg/mL was used for **d**. Scale bars represent 200nm for **a-c** and 100nm for **d**.

PNAG physically associated with OMVs. PNAG OMVs were subjected to density gradient ultracentrifugation to determine if PNAG remained OMV associated (**Figure 4.4**). During density gradient ultracentrifugation, macromolecules and particles migrate through a density gradient until buoyancy and sedimentation force reach an equilibrium. Liposomal nanoparticles like OMVs tend to be less dense than soluble macromolecules like proteins and polysaccharides due to their lipid content. By separating the PNAG OMV preparations by density, we showed that total protein content (**Figure4.4a**), PNAG content (**Figure4.4b**), and OmpA, an OMV specific protein marker (**Figure4.4c**) are all co-localized.

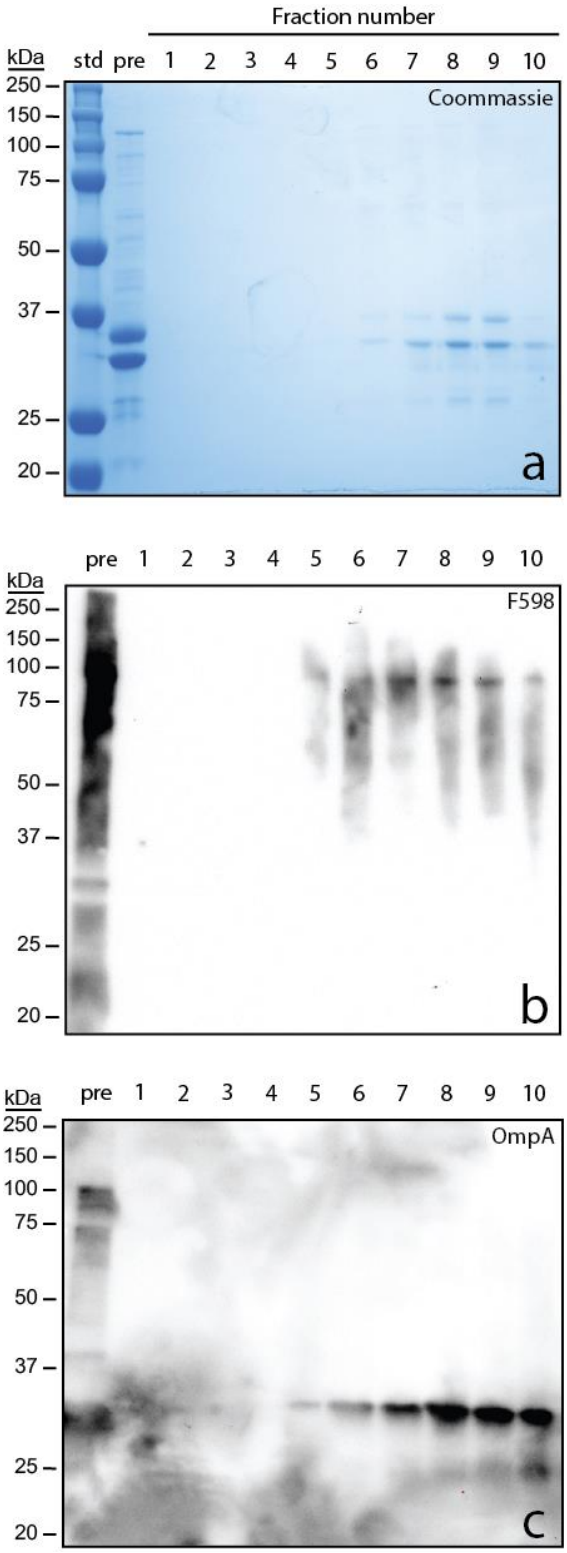

Figure 4.4: Density gradient ultracentrifugation of PNAG OMVs. OMVs from JC8031 cells with induced p*pgaABCD* were harvested an approximately 1mg of OMVs was subjected to density gradient ultracentrifugation using an Optiprep gradient. Discrete 0.5mL fractions were taken, and 10µL of each fraction was subjected to SDS-PAGE and analyzed by Coomassie stain (**a**) or western blot with F598 (**b**) or anti-OmpA (**c**). Numbers correspond to relative fraction density with 1 being the least dense and "pre" being the un-fractionated control.

Expressing *icaB* and knocking out *lpxM* does not affect the quantity of PNAG on OMVs. In previous studies where animals with immunized with PNAG, it was found that antibodies specific the de-acetylated form were responsible for protection. To shift the balance of the PNAG on our OMVs more toward the de-acetylated form, we heterologously expressed the PNAG de-acetylase, *icaB*, from *S. aureus* in our strain. This particular de-acetylase was chosen because it is not anchored membrane anchored like PNAG de-acetylases from Gram-negative species (i.e. *E. coli pgaB*). Rather it is membrane associated through binding to peptidoglycan[110]. To facilitate IcaB's expression in *E. coli*, we removed its native secretion signal sequence and replaced it with a Sec secretion sequence suitable for periplasmic expression in *E. coli* and added a C-terminal His_6 tag for ease of detection. Western blotting of both periplasmic and whole cell fraction of JC8031 expressing IcaB showed it was present as a soluble protein in the periplasm and that the majority of it was associated with the membrane containing whole cell fraction (**Figure4.5a**). In addition, we also modified the OMVs produced by our cells to be less toxic by knocking out *lpxM*, an acyl transferase that is responsible for fully assembling the sixth and final acyl chain onto Lipid A. It has been shown by the DeLisa Research Group and others that this modification of lipid A drastically reduces its reactogenicity, making OMVs that contain this modified lipid A more suitable for use in vaccination trials. Using PNAG specific dot blotting, we have shown that expression of *icaB*, knockout of *lpxM*, and a combination of those two modifications does not affect the abundance of PNAG on OMVs (**Figure4.5b**).

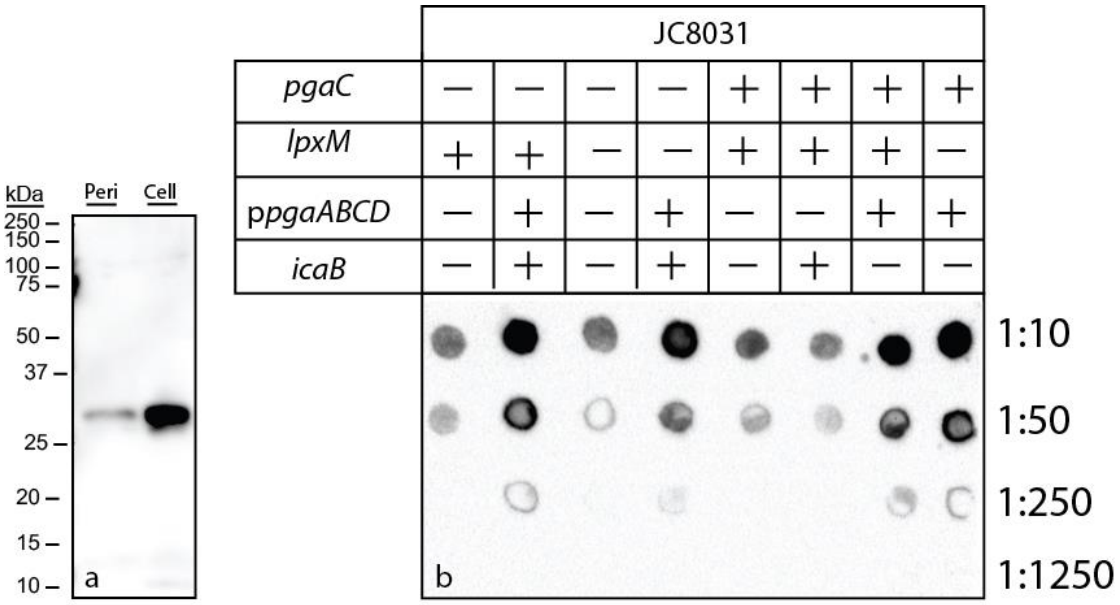

Figure 3: Expression of *icaB* and knockout of *lpxM* does not affect PNAG on OMVs. The expression of periplasmic and whole cell fractions of IcaB from JC8031 cells was visualized using anti-His via Western blotting (**a**). PNAG on OMVs from the listed strains (JC8031±Δ*pgaC*±Δ*lpxM* ±p*pgaABCD*±*icaB*) were visualized with F598 and anti-human secondary via dot blotting (**b**).

Mice vaccinated with PNAG OMVs produce glycan specific antibodies. Two immunization trials were performed on four-week-old female BALB/c mice to quantify the humoral immune response to different PNAG OMV formulations (**Figures 4.6,4.7**). As expected, PNAG specific IgG titers observed form mice immunized with polysaccharide alone (dPNAG) or OMVs from cells without p*pgaABCD* were not significantly higher than titers observed from negative control groups (PBS). During both rounds of immunization, it is easy to see that PNAG specific IgG titers increased over time and after multiple rounds of booster immunizations (**Figure 4.6**). During both trials, PNAG + IcaB OMVs produced the highest glycan specific antibody titers among OMV immunization groups. Those titers were significantly higher than the titers observed for empty OMVs in all cases ($p<0.05$). During the second trial, we found that knocking out *lpxM* had no significant effect on PNAG specific IgG titers (**Figure 4.6b**). An inconsistency between the two

rounds of immunization are the PNAG specific titers produced from mice immunized with the tetanus toxoid dPNAG oligomer. During the first trial, no mice showed any detectable anti-PNAG IgG while during the second trial, every mouse showed and PNAG specific IgG titer higher than the highest OMV case. We attribute this difference to possibility of variance in the production of tetanus toxoid glycoconjugate. We also compared the PNAG specific titers of other antibody subtypes in a subset of mice from each trial (**Figure 4.7**). The IgA antibody titers from the first trial were predictably low as circulating IgA concentration in the blood is known to be quite low when compared to the concentration of IgA in mucosal membranes, but the highest titers were from the group immunized with PNAG + IcaB OMVs (**Figure 4.7a**). The IgM titers from the first trial closely followed the trends for the IgG titers, with the exception that there was no difference between the PNAG OMVs and PNAG IcaB OMVs (**Figure 4.7b**). This result is not completely unexpected as IgMs have much broader binding capabilities than affinity matured IgGs. We examined the titers of IgG1 and IgG2a from every group in the first immunization and form a subset in the second immunization (**Figure 4.7c,d**). We found that the titers from OMV immunized groups followed the trends of total IgG titers and that there was no significant bias for one IgG subtype over another. The only significant bias was observed during the second immunization when mice immunized with the tetanus toxoid glycoconjugate showed an apparent IgG1 bias (**Figure 4.7d**).

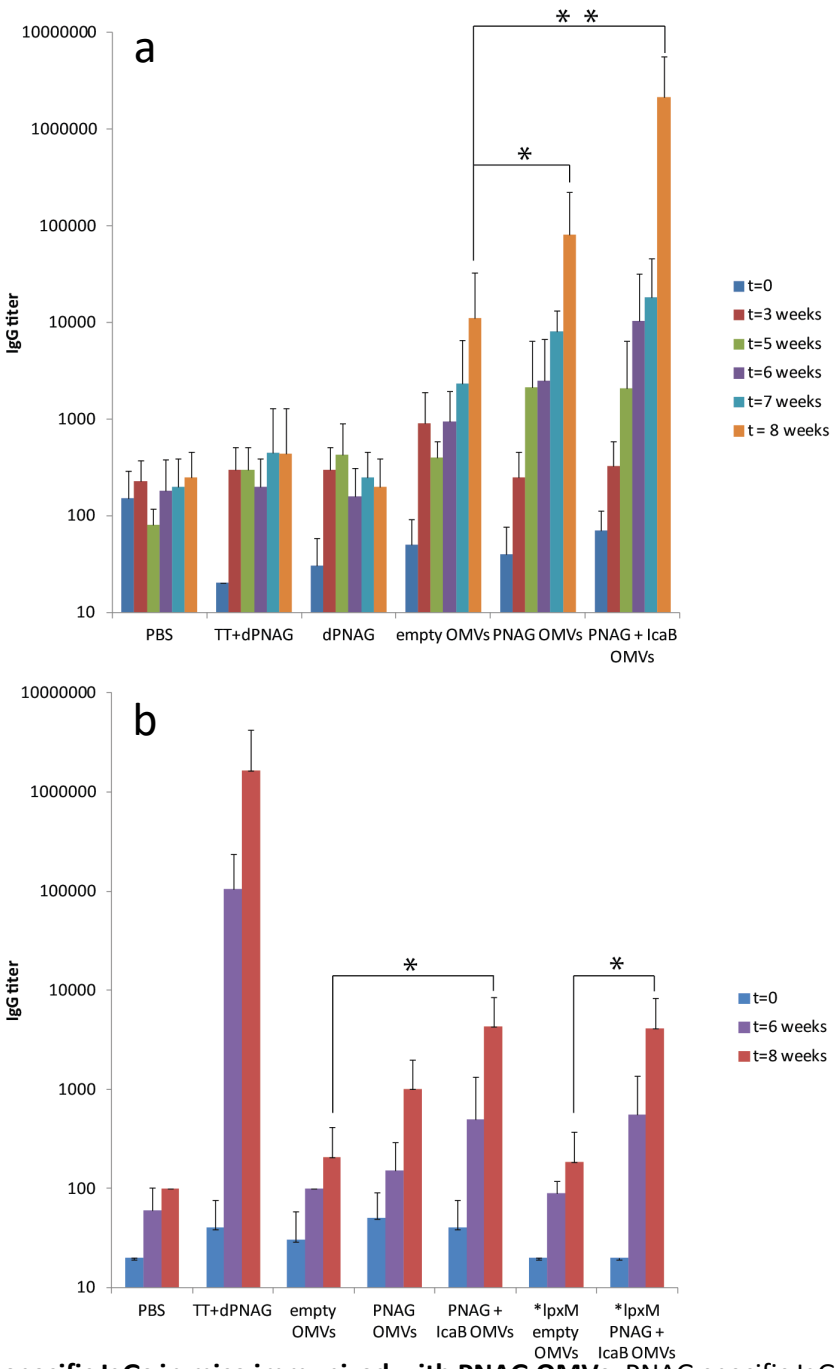

Figure 4: PNAG specific IgGs in mice immunized with PNAG OMVs. PNAG specific IgG titers from mice immunized with OMVs, tetanus toxoid glycoconjugate (TT+dPNAG), or dPNAG alone (dPNAG) 8 weeks after initial immunization. All OMVs were made in JC8031Δ*pgaC* background with two groups including the additional Δ*lpxM* knockout (**b** far right). Bars show the average + standard deviation of IgG titers in each group eight mice. The top panel (a) shows the titer results from the first round of OMV immunization while the bottom panel (b) shows the results from the second round. Mice immunized with OMVs were injected s.c. at t=0 and boosted at 3 and 6 weeks with 10µg total protein. Mice immunized with dPNAG were injected s.c. at t=0 and boosted at 3 and 6 weeks with 10µg dPNAG. Mice immunized with TT+dPNAG were injected s.c. at t=0 and boosted at 3 weeks with 10µg TT+dPNAG as measured by total protein content. The dPNAG and TT+dPNAG were administered with incomplete Freund's adjuvant. (*) and (**) represent statistical significance ($p<0.05$, $p<0.01$, respectively) by Tukey-Kramer HSD.

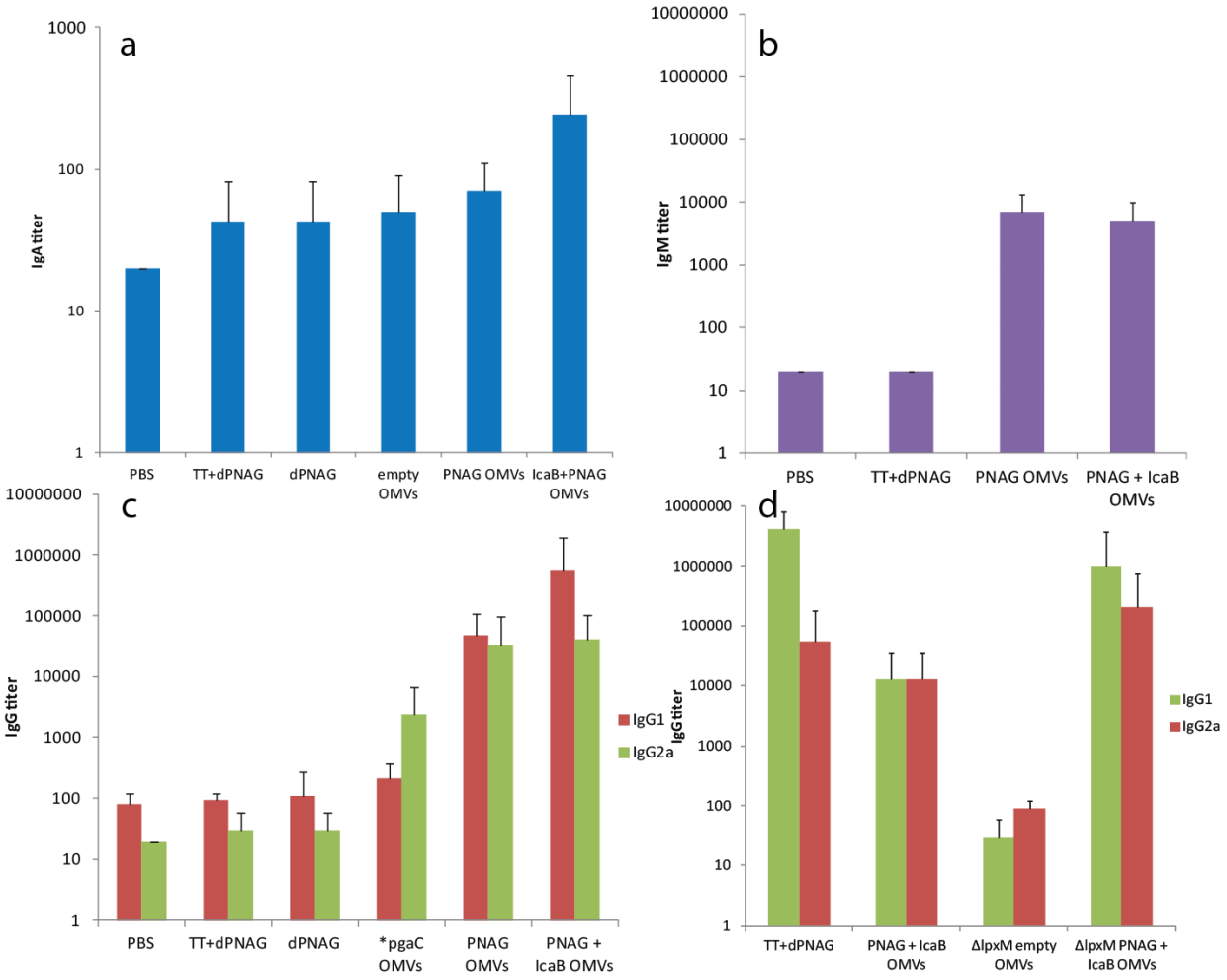

Figure4.7: Antibody subtype titers in mice immunized with PNAG OMVs. PNAG specific IgA (a), IgM (b), IgG1, and IgG2a (**c,d**) antibody subtype titers from mice immunized with OMVs, tetanus toxoid glycoconjugate (TT+dPNAG), or dPNAG alone (dPNAG) at week 7 (**a,b**) or week 8 (**c,d**) after initial immunization. All OMVs were made in JC8031Δ*pgaC* background with two groups including the additional Δ*lpxM* knockout (**d** far right). Bars show the average + standard deviation of subtype titers in each group of eight mice. The first three panels (**a-c**) show the titer results from the first round of OMV immunization while the last panel (**d**) shows the results from the second round. Mice immunized with OMVs were injected s.c. at t=0 and boosted at 3 and 6 weeks with 10µg total protein. Mice immunized with dPNAG were injected s.c. at t=0 and boosted at 3 and 6 weeks with 10µg dPNAG. Mice immunized with TT+dPNAG were injected s.c. at t=0 and boosted at 3 weeks with 10µg TT+dPNAG as measured by total protein content. The dPNAG and TT+dPNAG were administered with incomplete Freund's adjuvant. The only significant bias ($p<0.05$) in subtype titers was identified for mice immunized with TT+dPNAG between IgG1 and IgG2a during the second immunization (**d**, first group) as determined by Student's T-test.

PNAG OMVs provide partial protection against *S. aureus* challenge in mice. Groups of

Immunized mice (n=8) were challenged with ten times the modified LD_{50} of *S. aureus*

(Rosenbach ATCC 29213) via tail vein injection. At this dose, we expected to see no survivors in mice immunized with PBS, little to no protection in mice immunized with dPNAG alone or with any of the empty OMVs, and substantial to complete protection in mice immunized with the tetanus toxoid glycoconjugate or PNAG OMVs. Our observations when combining data from the two challenge experiments were consistent with our predictions. Mice immunized with PBS and empty *_lpxM_* OMVs had the lowest survival rates (<20%) while those immunized with dPNAG alone, empty OMVs, and PNAG OMVs had an intermediate level of survival (38%). Mice immunized PNAG+IcaB OMVs, PNAG+IcaB *_lpxM_* OMVs had the highest survival rate (50%) and were higher than the survival rate of the tetanus toxoid glycoconjugate positive control (42%) (**Table 4.3**). When comparing the Kaplan-Meyer survival curves of the individual groups in the first trial, we found that only PNAG+IcaB OMVs and TT+dPNAG provided significant ($p<0.05$) protection based on a log-rank score when compared to the PBS control (**Figure 4.8a, Table 4.1**). In the second trial, PNAG OMVs and PNAG + IcaB *_LpxM_* OMVs provided significant protection compared to the PBS control ($p<0.05$) while PNAG + IcaB OMVs were close to achieving significant protection ($p\approx0.08$) (**Figure 4.8b, Table 4.2**). It should be noted that survival rates of mice in groups immunized with TT+dPNAG was very different between the two trials (50% vs. 25% **Table 4.1,4.2**) and that the PNAG specific IgG titers were inversely related in the two studies (<10^3 vs. >10^5 **Figure 4.6**). Interestingly, mice immunized with empty OMVs had a different survival rate (38% survival **Table 4.1**) than mice immunized with empty*_lpxM_* OMVs (12.5% survival **Table 4.2**) while mice immunized with PNAG+IcaB OMVs showed the same survival rate as those immunized with PNAG+IcaB*_lpxM_* OMVs (50% **Table 4.3**). Additionally, expression of IcaB may have impacted survival rates as PNAG OMV

immunized mice survived at a rate of 38% and PNAG+IcaB OMV immunized mice had a survival rate of 50% (**Table 4.3**).

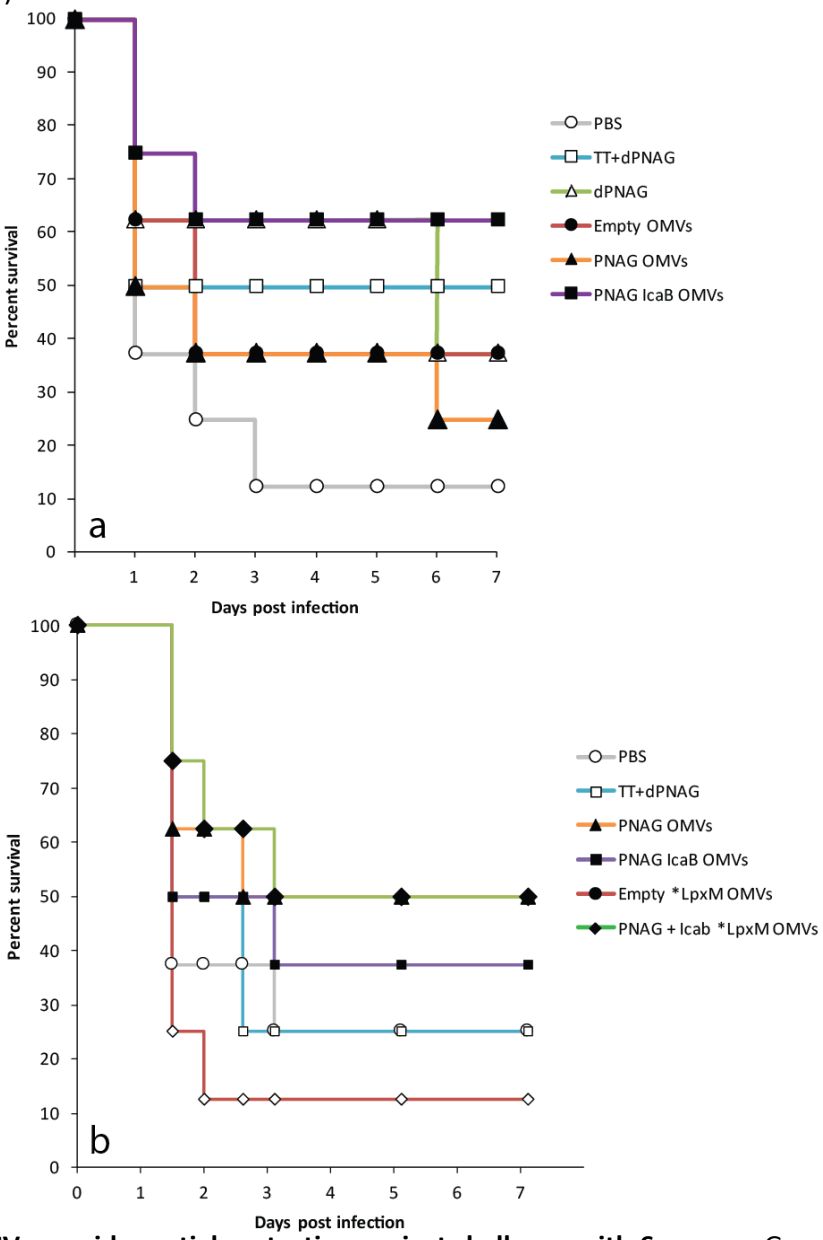

Figure 4.8: PNAG OMVs provide partial protection against challenge with *S. aureus*. Groups of mice (n=8 for except TT+dPNAG in **b** where n=4) were immunized with various OMV formulations and challenged with 10xmLD$_{50}$ of *S. aureus* (strain Rosenbach ATCC 29213;2*10^8 CFU/100µL) via tail vein injection. Mice were weighed thrice daily for the first 72 hours then once daily for the remain 4 days. Mice were euthanized if their weight dropped below 80% of weight at t=0 or if they became moribund. Mice immunized with OMVs were injected s.c. at t=0 and boosted at 3 and 6 weeks with 10µg total protein. Mice immunized with dPNAG were injected s.c. at t=0 and boosted at 3 and 6 weeks with 10µg dPNAG. Mice immunized with TT+dPNAG were injected s.c. at t=0 and boosted at 3 and 6 weeks with 10µg TT+dPNAG as measured by total protein content. The dPNAG and TT+dPNAG were administered with incomplete Freund's adjuvant. PNAG + IcaB OMVs and PNAG + IcaB **LpxM* OMVs showed a significant protection in both challenges over PBS ($p<0.05$) groups as measured by a log-rank test.

Table 4.1: Survival data for first challenge experiment

mouse immunization group	# of surviving mice at each day								% survival
	0	1	2	3	4	5	6	7	
PBS	8	3	2	1	1	1	1	1	12.5
TT+dPNAG**	8	4	4	4	4	4	4	4	50.0[1]
dPNAG**	8	5	5	5	5	5	3	3	37.5
Empty OMVs	8	5	3	3	3	3	3	3	37.5
PNAG OMVs	8	4	3	3	3	3	2	2	25.0
PNAG IcaB OMVs	8	6	5	5	5	5	5	5	62.5[1]

[1]Significant protection over mice immunized with PBS (p<0.05, log-rank test)
****Administered with incomplete Freund's adjuvant**

Table4.2: Survival data for second challenge experiment

mouse immunization group	# of surviving mice at each day							% survival
	0	1.5	2	2.625	3.125	5.125	7.125	
PBS	8	3	3	3	2	2	2	25.0
TT+dPNAG**	4	2	2	1	1	1	1	25.0
PNAG OMVs	8	5	5	4	4	4	4	50.0[1]
PNAG IcaB OMVs	8	4	4	4	3	3	3	37.5
Empty **lpxM* OMVs	8	2	1	1	1	1	1	12.5
PNAG + IcaB **lpxM* OMVs[1]	8	6	5	5	4	4	4	50.0[1]

[1]Significant protection over mice immunized with PBS (p<0.05, log-rank test)
****Administered with incomplete Freund's adjuvant**

Table4.3: Combined endpoint survival rates

mouse immunization groups	# of survivors	# of total mice	% survival
PBS	3	16	18.8
TT+dPNAG**	5	12	41.7
dPNAG**	3	8	37.5
Empty OMVs	3	8	37.5
PNAG OMVs	6	16	37.5
PNAG IcaB OMVs	8	16	50.0
Empty **lpxM* OMVs	1	8	12.5
PNAG + IcaB **lpxM* OMVs	4	8	50.0

****Administered with incomplete Freund's adjuvant**

Antibodies produced in PNAG OMV vaccinated mice show bactericidal activity against *F. tularensis*. To determine if sera harvest from mice immunized with PNAG OMVs contained antibodies with bactericidal activity against other bacterial species, we performed serum bactericidal assays (SBAs) using *F.* tularensis LVS. Our results show that sera from mice immunized with PNAG+IcaB OMVs had a concentration dependent bactericidal activity that is higher than sera from mice immunized with PBS and that the highest concentration of sera had killing activity equivalent to that of the positive control F598 (**Figure 4.9**). Interestingly, sera from PNAG+IcaB immunized mice also showed higher bactericidal activity than sera from mice immunized with empty OMVs at lower serum concentrations (1/270,1/90), but that difference is greatly reduced at higher serum concentrations (1/30,1/10). Lastly, the serum from mice immunized with TT+dPNAG had a highly variable bactericidal activity with two mice's sera showing effectively no bactericidal activity and two others' showing complete killing at all concentrations.

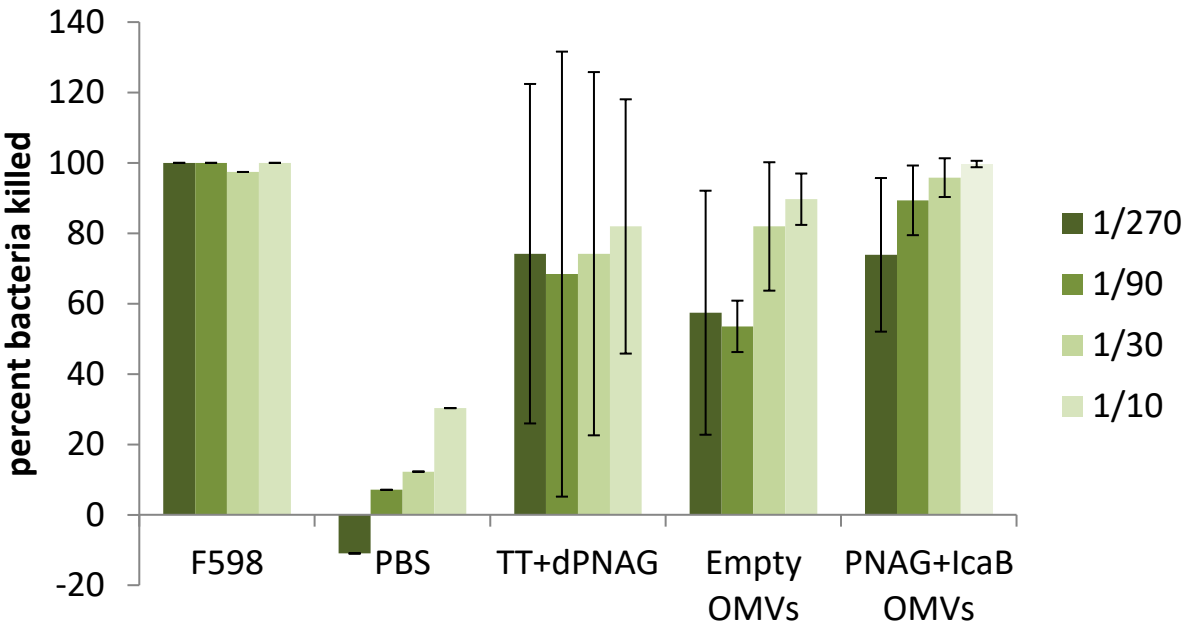

Figure 4.9: Serum bactericidal assay against *F. tularensis* LVS using serum from PNAG immunized mice. Data above shows percent LVS killed in SBA relative to killing by baby rabbit complement alone. Various dilutions of sera samples were used to show concentration dependent effects. The human monoclonal F598 was used as a positive control for bactericidal activity and was also diluted according to shown dilution scheme with 1:1 being equivalent to 1mg/mL. Values shown are averages of technical duplicates and biological replicates within immunization groups. The number of mice in each group are PBS n=1, TT+dPNAG n=4, Empty OMVs n=2, PNAG + IcaB OMVs n=8, and F598 monoclonal antibody n=1. Vertical bars represent the average bactericidal activity of sera samples within an immunization group. Error bars represent standard deviations of individual sera activities (TT+dPNAG, Empty OMVs, PNAG+IcaB OMVs) or range of technical duplicates of single samples (F598 and PBS).

Discussion

Here, we have shown that secreted, extracellular polysaccharide, PNAG, is enriched in OMV samples prepared from hypervesiculating strains and that amount of the polysaccharide can be augmented through overexpression of its native biosynthetic pathway. We have also shown through TEM that the lack of or overabundance of PNAG production does not affect the morphology of OMVs produced by the same cells. Though the presence of PNAG may form partially insoluble aggregates that contain OMVs, the entire samples remains in a colloidal suspension. Immunostaining of dilute OMV samples with gold nano-particles allowed us to visualize PNAG decorating OMVs, and density gradient ultracentrifugation showed that PNAG remains OMV associated even when the PNAG and OMV have different forces applied to them. Additionally, we showed that PNAG on OMVs is unaffected by the additional expression of a PNAG deacetylase from *S. aureus* (IcaB), the modification of the lipid A structure in the outer membrane via deletion of *lpxM*, and the combination of both these modifications. We have successfully created a non-canonical glycoconjugate OMV vaccine displaying PNAG through a wholly biosynthetic process.

We showed that our PNAG OMVs were able to elicit a strong PNAG specific IgG response in mice. This significant humoral immune response was consistent across two immunization trials. The antibodies produced by PNAG+IcaB OMVs were produced at a higher titer than PNAG specific antibodies produced by PNAG OMVs alone in both trials, though the difference was only significant in the first trial ($p<0.05$). The consistency of these responses is highlighted by the inconsistency of response to the tetanus toxoid glycoconjugate. Previous studies have shown that this glycoconjugate has produced significant anti-PNAG titers in mice,

but it's variability in our hands raises some concerns over how consistently immunogenic it is. We also showed that there was no significant difference in glycan specific IgG titers between mice immunized with PNAG+IcaB OMVs and mice immunized with PNAG+IcaB *_lpxM_* OMVs, adding to the growing pool of data that this deletion does not affect the immunogenicity of OMVs but does reduce their reactogenicity.

The titers of glycan specific antibody subtypes (IgA, IgM, IgG1, and IgG2) followed the trends of total glycan specific IgGs in the round of immunization with the exception of IgM titers. There was no significant difference in PNAG specific IgM titers in mice immunized with PNAG OMVs and PNAG+IcaB OMVs. This result is not unexpected as IgMs tend to have a broader specificity than more mature subtypes and may not be able to distinguish the subtle difference between degrees of acetylation on PNAG polymers. The PNAG specific IgA titers are low as to be expected when examining IgA concentration in blood, but PNAG+IcaB OMVs do have the highest titer among immunization groups. The PNAG specific IgG1 and IgG2a response generated by OMVs in both immunizations show no bias for either subtype which is consistent with previous observations[111]. Conversely, we saw the expected significant bias for IgG1 in mice immunized with the tetanus toxoid glycoconjugate[106, 112]. A bias of IgG1 over IgG2a is representative of a Th2 immune response which tends to act more through the humoral route of adaptive immunity while an IgG2a over IgG1 bias implies a Th1 immune response which tends to act more through the cellular arm of the immune response. Protein glycoconjugates are known to produce a Th1 biased immune response while evidence is mounting that glycOMVs induce a more balanced hybrid Th1 and Th2 response[14-16]. The type of immune response generated by OMV vaccines is important as it can predict the effectiveness of the

vaccine against a particular pathogen. The pathogen *S. aureus*, for example, is successfully cleared through both responses[113, 114].

Our challenge experiments were showed significant protection against challenge with *S. aureus* when compared against PBS immunized mice. Mice immunized with PNAG+IcaB OMVs had the highest survival rate at 50%. In a result which maps directly back to IgG titers, the *lpxM* deletion did not affect the survival rates. Perhaps the most confusing and unexpected results are the inconsistencies between the trials *vis-a-vis* the TT+dPNAG immunization groups. In the first trial, mice immunized with TT+dPNAG generated no detectable glycan specific immune response among any of the antibody subtypes, yet the mice had a survival rate of 50% during the challenge. In the second trial, mice immunized with TT+dPNAG had the highest PNAG specific IgG titers recorded throughout the study, but only had a survival rate of 25%. These inconsistencies led us to investigate whether there was a correlation between antibody titers and survival in individual mice. After mapping survival data to PNAG specific titers, we saw no correlation between mice that survived and mice that had the highest IgG titers or individual mice that may have had a slight IgG1 vs. IgG2a subtype bias. This result implies that antibody titer alone is not a sufficient measurement for the success of a vaccine against *S. aureus*, and that the cellular immune response is also likely to be crucial to protection against *S. aureus.* This result was mirrored in our SBA against *F. tularensis* LVS.

As we previously discussed, though PNAG was first identified as a virulence factor in *S. aureus*, it present on a wide range of human pathogens[97, 115]. Our collaborator Gerald Pier has shown that PNAG is present on the surface of *F. tularensis* (unpublished), we have shown that a human monoclonal antibody against PNAG (F598) is able to completely kill *F. tularensis*

LVS in a SBA. We have also shown that sera from mice immunized with PNAG+IcaB OMVs also has complete bactericidal activity, albeit at higher concentration than the F598. Interestingly, sera from mice immunized with empty OMVs also showed bactericidal activity against *F. tularensis* LVS at higher concentrations. This result, combined with previously observed results from studies with glycOMVs, support the hypothesis that OMV chassis alone is able to provide a broad spectrum, non-specific, defense against pathogens. We hypothesize that the OMV chassis can serve to "prime" the immune response in an as yet uncharacterized manner, though our SBA experiments tend to suggest this non-specific priming is at least partially humoral. Similar the results observed from the survival data, individual IgG titers do not correlate with bactericidal activity. This lack of correlation is most dramatic when observing the bactericidal activity of sera from mice immunized with TT+dPNAG. All mice had exceptionally high PNAG specific IgG titers (>10^5), but sera from two of them showed almost no bactericidal activity. This observation further supports the conclusion that IgG titers alone are insufficient to predict the success or failure of a vaccine candidate.

Future immunization studies using PNAG OMVs against *S. aureus* should be conducted using larger immunization group sizes. As the measured difference between negative control (PBS immunized mice) and most positive experimental case (PNAG+IcaB OMVs) is relatively small in the context of this challenge model, yielding a hazard ratio of only 2.5. The initial experiment design assumed a hazard ratio of 18 which would have been the equivalent of 7/8 mice surviving in the immunized groups and <1/8 mice surviving in the PBS groups. With the observed hazard ratio of approximately 2.5, we would need the sample size to increase to roughly 70 mice per group to achieve statistical significance[116]. Additionally, examining the

cellular response to PNAG OMVs would be valuable. By extracting splenocytes from immunized and naive mice, we could measure the production of cytokines such as IL4, IL8, and TNF-α in distinct subpopulations of cells in response to stimulation with PNAG alone, empty OMVs, and PNAG OMVs to elucidate how and which cells of the immune response may be responsible for the partial protection we have observed.

As PNAG is a prevalent on a wide variety of bacterial pathogens, we should test our current PNAG OMVs as vaccines against several other pathogens known to display PNAG on their surfaces. These pathogens could include several Gram-positive species such as *Streptococcus pyogenes, Streptococcus pneumoniae,* and *Streptococcus agalactiae* as well as Gram-negative species such as *Salmonella enterica*, *Helicobacter pylori*, or pathogenic strains of *E. coli*. In addition to further *in vivo* testing, we could more rapidly evaluate the protection using *in vitro* bactericidal assays and sera currently in stock from the second immunization trial. The first of these assays would be an opsonization and phagocytotic killing assay (OPKA) against *S. aureus* We would expect results from this assay to mirror what was seen during the challenge trial. We could then expand the range of pathogens rapidly using SBAs for the Gram-negative pathogens and OPKAs for the Gram-positives.

Materials and Methods

Bacterial strains and plasmids. The strains and plasmids used in this chapter are described below (**Table4.4**). Briefly strains are based on the well-known hypervesiculating strain JC8031 whose phenotype is attributed a knockout of *tolRA*. Plasmid features are outlined below. The *S. aureus* PNAG deacetylase IcaB was amplified from genomic DNA and modified to contain a

DsbA signal sequence for periplasmic targeting and His tag for detection before being ligated in the pTrc99a expression vector. The pathogenic strain of *S. aureus* used is the Rosenbach strain (ATCC 29213) and was cultured in liquid LB just as *E. coli*. It was, however, grown on high salt LBA (5% NaCl) which is selective against a broad range of possible contaminants. LVS was cultured in Modified Mueller Henton broth (MMH, Mueller Henton broth supplemented with 2% IsoVitaleX) overnight (closer to 24 hours) with shaking at 37˚C (Note: the key to liquid cultures of *F. tularensis* LVS is a high starting density). The saturated culture was then sub-cultured 1:50 in MMH and grown to mid-log phase (about 3 hours). Sealed 96-well plates were used to measure the OD_{600nm} against MMH blank and the density determined using the previously described expression for CFU LVS per OD_{600} per mL (4.9*10^6 CFU/mL/OD_{600}). Bacteria were pelleted at 6,000xg for 5 minutes and washed with sterile PBS before being resuspended at a density of 10^5 CFU/mL in PBS for using the SBA.

Creation of hypervesiculating PNAG knockout strains via P1 transduction. Briefly, donor phages were created by incubating P1 phage with the member of the Keio collection that contains the *pgaC* gene knocked out by a kanamycin resistance cassette[93]. After complete lysis of the donor culture, phage sample was clarified via centrifugation and stored at 4˚C until used. These phages were incubated with JC8031 and JC8031*ΔlpxM* for 30 minutes at 37˚C. Lysis of the recipient culture by phage was halted via the addition of 1mM sodium citrate before the cells were pelleted and plated on kanamycin and sodium citrate. Several colonies were restreaked on kanamycin and sodium citrate to verify removal of persistent phage.

PNAG OMV preparation. OMVs were prepared as previously described in this work. Briefly, plasmids containing the necessary genes for production of PNAG and/or IcaB (**Table 2.1**) were transformed into appropriate hypervesiculating strains using electroporation. Transformed cells were selected on medium supplemented with the appropriate antibiotic. An overnight culture

of a single colony was selected and grown overnight in LB medium. Saturated overnights were subcultured 1:100 in LB supplemented with appropriate antibiotics. The cultures were grown to mid-log phase ($OD_{600} \approx 0.6$) at which point, PNAG biosynthesis and IcaB expression were induced with IPTG (0.1 mM). Induction was allowed to proceed for 16-20 hours at 37˚C. Cells were pelleted via centrifugation at 10,000xg for 10 minutes. Cell-free culture supernatants were collected post induction and filtered through a 0.2 μm filter. Vesicles were isolated by ultracentrifugation (Beckman-Coulter; TiSW28 rotor; 141,000xg; 3 h; 4˚C) and resuspended in sterile PBS. OMVs were quantified by the bicinchoninic-acid total protein assay (BCA Protein Assay; Pierce) using BSA as the protein standard.

Western and dot blotting. Whole cell and OMV samples were prepared for SDS-PAGE analysis by boiling for 15 min and cooling to room temperature in the presence of loading buffer containing β-mercaptoethanol. Samples were run on 10% cross-linked polyacrylamide gels (BioRad, MiniPROTEAN® TGX) and transferred to a PVDF membrane via semidry transfer. For dot blots, 5μL of untreated cells and OMVs were spotted directly onto nitrocellulose membrane. After blocking with a 5% milk in Tris-buffered saline (TBS), membranes were probed with HRP-conjugated anti-His (Abcam) for the detection of IcaB in the periplasm. When analyzing samples for the presence of PNAG, membranes were first probed with the human monoclonal IgG F598 (graciously provided by Gerald Pier) and visualized with anti-human HRP-conjugated secondary (Promega) [110]. When analyzing density gradient samples for OmpA, membranes with stained with mouse anti-OmpA (graciously provided by Wilfred Chen) before being visualized with anti-human HRP-conjugated secondary (Promega). Total protein in OMV fractions was visualized via non-specific protein stain (R250 BioRad). Signals were visualized

using HRP substrate Clarity ECL (BioRad) or white light transillumination and were imaged with a ChemiDoc XRS+ Imaging System (BioRad).

Dispersin B treatment of PNAG OMVs. To further ensure that the observed signals from F598 binding are caused by OMV associated PNAG, samples were subjected to enzymatic treatment with DispersinB. DisperinB is an enzyme the very specifically degrades the β-1-6 glycosidic bond in PNAG and was purchased from Kane Biotech Inc [117]. The OMVs from JC8031 ±p*pgaABCD* were diluted to 80μg/mL in PBS and treated with or without 50μg/mL DispersinB at 37^{o}C for 24 hours. Samples were dot blotted similarly to those described previously [100].

TEM of PNAG OMVs. Electron microscopy. Structural analysis of vesicles was performed via transmission electron microscopy as previously described[13]. Briefly, vesicles were diluted to 100μg/mL and negatively stained with 2% uranyl acetate and deposited on 400-mesh Formvar carbon-coated copper grids. Immunostaining of PNAG on OMV surfaces was performed as previously described[97]. Briefly, OMVs were diluted to 10μg/mL and deposited on 400-mesh Formvar carbon-coated copper grids. Deposited OMVs were then blocked with TBS containing 5% BSA. Blocked grids were then incubated at room temperature F598, washed, and incubated with anti-human gold-nanoparticle-conjugated antihuman secondary (Sigma). Imaging of both types of samples was performed using a FEI Tecnai T-12 SPIRIT transmission electron microscope.

Density gradient ultracentrifugation of PNAG OMVs. To ensure that the PNAG detected on OMVs was tightly bound, they were subjected to density gradient ultracentrifugation as previously described [88]. Briefly, OMVs were suspended in HEPES buffer (pH=6.8) instead of PBS and diluted into Optiprep solution to a final concentration of 1.0mg/mL in 1.5mL of 45% Optiprep solution in HEPES. Discrete layers of Optiprep/HEPES were added to a 12mL

ultracentrifuge tube by carefully pipetting more dense layers below less dense layers. Each layer was added in 330µL fractions with the following % composed of Optiprep: 10%, 15%, 20%, 25%, 30%, 35%, 1.5mL OMV fraction containing 45% Optiprep, 9.0mL of 60% Optiprep to fill the tube. The gradients were spun at 180,000xg for 3 hours after which thirteen 0.5mL fractions were taken from the top of the centrifuge tube. The samples were subjected to SDS-PAGE and analyzed by Western blot for the presence of PNAG and OmpA.

Preparation of PNAG. The purification of PNAG from *E. coli* was performed by modifying a combination of two previously described methods[103, 118]. The Top10 strain of *E. coli* which lacks endogenous production of PNAG, was transformed with p*pgaABCD,* and subcultured in LB containing tetracycline to mid-log phase. Production of PNAG was stimulated with IPTG and the cells were cultured for an additional 16 hours after which point they were pelleted via centrifugation at 10,000xg for 10 minutes. The supernatant was recovered and filtered through a 0.2µm filter before being concentrated 25x in a 3kda MWCO concentration column (Millipore). PNAG was then precipitated from solution via the addition of 2 volumes of 200 proof ethanol. Insoluble PNAG was recovered by gentle centrifugation <1,000xg for <5min and the supernatant was discarded. The PNAG pelleted was partially resuspended in PBS (1:50 original supernatant volume) and incubated overnight in 10µg/mL lysozyme and 10µg/mL DNAse I at 37˚C. The peptidoglycan and DNA digested PNAG was then subjected to 0.1mg/mL proteinase K treatment overnight at 37˚C. The isolated PNAG was then dialysed into water to remove digested peptides and nucleotides using a 5kDa Slide-a-lyzer cassette (Thermo) before being lyophilized. To facilitate removal of acetyl groups from PNAG, it was resuspended in 5M NaOH and allowed to incubate overnight at 37˚C. The basic solution was then neutralized via

addition of an equal volume of 5M HCl, and the deacetylated PNAG was once again dialysed into water prior to a second lyophilization. The mass of recovered PNAG was quantified and used to make a 1mg/mL solution in PBS. The purity of this sample was evaluated using a Bradford total protein assay[119] as was determined to have <1% contaminating protein by mass.

Determination of mLD_{50} for *S. aureus* via tail vein injection. Due to ethical considerations, we have decided to use the modified LD_{50} (mLD_{50}) for our challenge with *S. aureus* (Rosenbach ATCC29213). The mLD_{50} differs from the LD_{50} in that the disease is not allowed to progress to death. Mice are preemptively euthanized when they reach pre-selected clinical thresholds. We used weight loss (<80% initial weight) and moribundity as clinical end points for our trials. Though we do not know the mLD_{50} for this pathogen in this animal model, we expected it to be similar to previously reported LD_{50}'s for similar models[28, 120]. We therefore only used a small number of doses (10^6, 10^7, and 10^8 CFU/mL) and a small number of mice in each dosing group (n=8). Twelve-week-old female BALB/c mice were administered 200µL of each of the above doses via tail vein injection. We observed that at 10^8 CFU/mL, exactly 50% of the mice were unable to clear the infection, making it our putative mLD_{50}. The protocol number for all animal trials performed in this work is (2012-0132) and was approved by the Institutional Animal Care and Use Committee at Cornell University.

Mouse immunization and challenge with *S. aureus*. We performed a power analysis to determine the appropriate group size [116]. For this analysis, we assumed a Type I error rate of 20%, implying a 1:5 chance of inappropriately evaluating a mouse as "protected". We assume a type II error rate of 5%, meaning we expected at most a 1:20 chance of inappropriately calling a

mouse "sick". We decided to dose the mice at 10xmLD_{50} to ensure a high hazard ratio, meaning we expected all the mice in unimmunized group to succumb to infection (only 5% survival). We expected survival rates of vaccinated mice to relatively high (90% survival). These assumptions yield a hazard ratio of 18. Based on these assumptions and immunization group sizes, we expected 47.5% of all mice to survive challenge.

A group size of n=8 mice was predicted to be sufficient for achieving significant protection in this challenge model. Four-week-old female BALB/c mice were immunized subcutaneously with 100µL injections of saline control (PBS), adjuvanted purified PNAG, adjuvanted tetanus toxoid conjugated to a pentamer of deacetylated PNAG (kindly provided by Gerald Pier), or one of the OMV formulations. Each dose represented 10µg of material as determined by total mass in the case of purified PNAG, and total protein content as determine by BCA in all other cases. Adjuvanted samples were formulated with incomplete Fruend's adjuvant (30% vol/vol) obtained from Sigma. Mice were boosted at 3 weeks and again at 6 weeks with the same doses. Blood was collected from each mouse from their mandibular sinus immediately before initial immunization and every subsequent week during the first immunization trial. During the second immunization trial, blood was only collected prior to each immunization and challenge. Additionally, a subset of mice in the second trial were euthanized prior to challenge to obtain larger blood samples via cardiac puncture.

Immunized mice were challenged with 10xmLD_{50} (10^9 CFU/mL) in 200µL of sterile PBS. Mice were weighed prior to challenge to establish an intervention weight when we would euthanize them (<80% initial weight). Mice were observed thrice daily for the first 72 hours then once daily for the remainder of the trial. During the first 24 hours, most mice were

euthanized based on moribundicity or at the urging of Cornell Center for Animal Resources and Education (CARE) veterinary staff. After 36 hours, we began to euthanize mice whose weight loss indicated severe bacteremia.

Enzyme-linked immunosorbent assay (ELISA) Glycan-specific antibodies produced in immunized mice were measured via indirect ELISA using a modification of a previously described protocol[13, 97, 106, 112]. Briefly, sera were isolated from the collected blood draws after centrifugation at 2,200*xg* for 10 min and stored at -20˚C. 96-well plates (Maxisorp; Nunc Nalgene) were coated with purified PNAG (25 μg/mL in PBS pH 7.4) and incubated overnight at 4°C. All PBS used was at pH 7.4. The next day, plates were washed 3 times with PBST (PBS, 0.05% Tween-20, 0.3% BSA) and blocked overnight at 4°C with 5% nonfat dry milk (Carnation) in PBS. Samples were serially diluted by a factor of five, in triplicate, between 1:100-1:7,812,500 in blocking buffer and added to the plate for 2 h at 37°C. Plates were washed 3 times with PBST and incubated for 1 h at 37°C in the presence of one of the following horseradish peroxidase-conjugated antibodies depending on which antibody subtype was being assayed: goat anti-mouse IgG (1:10,000; Abcam), anti-mouse IgG1 (1:10,000; Abcam), or anti-mouse IgG2a (1:10,000; Abcam), anti-mouse IgM (1:10,000; Abcam), or anti-mouse IgM (1:10,000; Abcam). After 3 additional washes with PBST, 3,3’-5,5’-tetramethylbenzidine substrate (1-Step Ultra TMB-ELISA; Thermo Scientific) was added and the plate was incubated at room temperature for 30 min. The reaction was halted with 2M H2SO4. Absorbance was quantified via microplate spectrophotometer (Molecular Devices) at a wavelength of 450 nm. Serum antibody titers were determined by measuring the lowest dilution that resulted in signal three standard deviations

above background. Statistical significance was determined using Tukey-Kramer post-hoc honest significant difference test and compared against the empty OMV control cases.

Serum bactericidal assay (SBA). The serum bactericidal assay was a modified version of previously reported protocols[97, 121, 122]. Previously aliquoted baby rabbit complement (Cedarlane) stored at -80˚C was used for this assay. An aliquot of heat inactivated complement (56˚C for 30 minutes) was also used as a control. Both active and inactive complement were thawed gently at room temperature and immediately placed on ice prior to use in the assay. For the experiment to determine optimal assay conditions, the complement concentration was varied in 1% increments from 0% to 10%. Serum samples from each mouse heat inactivated via incubation at 56˚C for 30 minutes prior to use. The human monoclonal F598 (1mg/mL) antibodies was used as positive controls for bactericidal activity. Serum was diluted 1:2 in sterile PBS and then serially diluted 1:3 three times to maximum dilution factor of 1:54 before being diluted 1:5 in the assay (final concentration range 1:10-1:270). The assay was performed in sterile 96-well plate in a biosafety cabinet.

For the optimization experiment, the assay began by adding 90µL of appropriately diluted baby rabbit complement or heat inactivated complement to each well. Then, 10µL of 10^5 CFU/mL *F. tularensis* LVS were added to each well. The plates were incubated at 37˚C with 5% CO_2 for 30 minutes. Every six minutes beginning at t=0, 10µL of each reaction was spotted on cysteine heart agar + 9% sheep's blood and allowed to trail down the half the length of the plate to facilitate colony counting. Plates were then incubated overnight at 37˚C with 5% CO_2 and colonies were counted the following day to determine optimal incubation time and complement concentration.

The optimal conditions for the SBA were determined to be 6% BRC and 30 minutes' incubation time. For each assay, 10µL of appropriately diluted serum was added to 6% BRC, 6% heat-inactivated BRC, or sterile PBS. To start the assay, 5µL of 10^5 CFU/mL *F. tularensis* LVS were added to each well. After 30 minutes incubating at 37°C with 5%CO_2, 10µL of the reaction mixes were spotted on cysteine heart agar + 9% sheep's blood and allowed to trail down the half the length of the plate to facilitate colony counting. Plates were then incubated overnight at 37˚C with 5%CO_2 and colonies were counted the following day to determine optimal incubation time and complement concentration.

Table4.4: Bacterial strains and plasmids used in this chapter.

Strain	Genotype	Source
-*S. aureus*	Rosenbach	ATCC 29213
-*F. tularensis*	LVS	Bradley Jones
-JC8031	*supE hsdS met gal lacY tonA ΔtolRA*	[85]
-JC8031Δ*lpxM*	detoxified lipid A	[16]
-JC8031Δ*pgaC::kan*	no endogenous PNAG production with hypervesiculation; kan	This study
-JC8031Δ*lpxM*Δ*pgaC::kan*	no endogenous PNAG production with modified lipid A in a hypervesiculating strain; kan	This study
-Top10	strain lacking endogenous PNAG production	Thermo Fisher
Plasmid	Description; Resistance marker	
pTrc99a	IPTG inducible expression vector; Amp	Lab stock
p*pgaABCD*	IPTG inducible expression vector; Tc	Gerald Pier
pTrc99a-IcaB	IPTG inducible expression vector for periplasmic expression of IcaB; Amp	This study

CHAPTER 5

DISCUSSION AND FUTURE DIRECTIONS

Discussion

In this work, we have made significant progress toward the creation of novel glycoconjugate vaccine candidates as well detailing general methods which can be used to develop and even wider range of vaccine candidates. We have shown successful glycoengineering of *E. coli* on several different scales. First, through metabolic engineering of hexosamine metabolism, we were able to use a GlcNAc salvage pathway to make *E. coli* glycobiology compatible with well-characterized, bioorthogonal azide-phosphine chemistry. We were able to use this chemistry on live *E. coli* cells displaying azide-labeled lipid-linked glycans via fluorescence flow cytometry. Next, we created a glycoengineered hypervesiculating strain that was able to produce vesicles loaded with lumenal glycoproteins containing the *F. tularensis* O-antigen. Though these glycoprotein containing OMVs are suitable vaccine candidates for *F. tularensis*, they contained mostly short oligomers of O-antigen subunits. To overcome this limitation, we also developed a method for conjugating full-length O-antigen oligomers to ClyA via *in vitro* protein glycosylation. Glycoprotein containing OMVs produced through either method are intact liposomes and suitable for use in immunization trials.

We also glycoengineered *E. coli* to produce a non-canonical glycoconjugate OMV vaccine through the overexpression of the PNAG biosynthesis pathway in a hypervesiculating strain. We showed that the morphology of OMVs produced from such a strain are unaffected, and that PNAG is localized to the surface of those OMVs. It was known that PNAG was both secreted into the culture media *E. coli* and that some fraction remained bound to the outer

surface of cells, but we were the first to show that it is also associated with OMVs. We also showed via density gradient ultracentrifugation that this physical association is strong enough to resist separation by different drag and buoyant forces. In preparation for using these PNAG OMVs in an animal model, we further modified them by producing them in strains expressing a PNAG deacetylase from *S. aureus* and by knocking out an acyltransferase to make the OMVs less reactogenic. These modifications had no impact on the amount of PNAG displayed on the OMVs. The PNAG+IcaB**lpxM* OMVs were able to produce a PNAG specific IgG humoral immune response and were provided better protection against *S. aureus* than mice immunized with an adjuvanted tetanus toxoid PNAG glycoconjugate. We also showed that sera from mice immunized with PNAG+IcaB OMVs had bactericidal activity against and attenuated strain of *F. tularensis*. This bactericidal activity against two vastly different bacterial pathogens speaks to the possibility of using PNAG+IcaB OMVs as a single subunit vaccine against multiple pathogens.

As mentioned previously in this work, there is no current satisfactory explanation for the glycan specific immune responses generated by immunization with glycOMVs such as the PNAG OMVs used herein[15, 16]. This uncertainty stems from the fact that polysaccharides are generally T-cell independent antigens. Except for a specific case involving a zwitterionic polysaccharide, carbohydrate antigens are generally not displayed on MHCII by professional antigen presenting cells. Our current hypothetical model for how the adaptive immune system responds to polysaccharides on OMVs is inspired by the current model for the generation of glycan specific antibodies in response to protein glycoconjugates. In this model, a naive B-cell with a glycan specific BCR binds the glycan component of the glycoprotein and subsequently endocytoses the entire molecule. As a professional antigen presenting cell, the B-cell digests

the glycoprotein and loads peptide fragments onto MHCII where they are presented to naive T-cells which may have a TCR that binds the displayed peptide, resulting in the formation of an immune synapse. An important point to note here is that the displayed peptide need not contain the glycan to form a successful synapse. Indeed, due to size limitations of the MHCII binding cleft, it is likely that the peptide responsible for the immune synapse is from a portion of the protein that does not contain the glycan[36]. It is possible for a glycOMV to stimulate the formation of immune synapses in the same way.

The glycOMV is a liposome nano-particle, ranging in diameter from 50nm to 250nm or larger. The smaller end of this size range (<100nm), which represents the majority of the glycOMVs, is well within the endocytotic capability of a professional APCs such as a naive B-cell[123]. If a naive B-cell with glycan specific BCR encounters a cognate glycOMV, the BCR will oligomerize causing subsequent endocytosis of the entire glycOMV nanoparticle. As a professional APC, the B-cell will digest and process the OMV as well as all of its endogenous protein cargo. As there are many proteins found in OMVs that have strong TCR binding epitopes, forming an immune synapse with a T-cell should be guaranteed[14]. It is through this co-localization of BCR epitope (the glycan) and TCR epitopes (endogenous OMV proteins) that we hypothesize glycOMVs are able to generate glycan specific antibodies. In this way, glycOMVs must be intact liposomes as simply mixing the carbohydrate antigen of interest with OMVs would not guarantee co-delivery to the same naive B-cell.

Future Directions

Use of Azide-linked sugars on OMVs to create small molecule conjugates. By creating OMVs displaying azide-linked glycans, we can functionalize OMVs so that any antigen of interest can be attached to them. By also using OMVs without azide-linked glycans on their surface as a control in immunization experiments, we could then have two samples: one sample in which co-delivery is guaranteed by bioorthogonal chemistry between the antigen of interest and azide labeled glycans and a second sample where the antigen of interest is not co-delivered with OMV antigens. This second sample controls for the innate immunostimulation caused by OMVs. This approach could be used directly with PNAG OMVs engineered to use the GlcNAZ compatible salvage pathway discussed in Chapter 1. As UDP-GlcNAc is the substrate used for PNAG biosynthesis, by overexpressing only *pgaACD* along with the GlcNAZ salvage pathway, we could produce fully acetylated PNAG on OMVs. We expect that by feeding these cells Ac_4GlcNAz, we will optimize the amount of azide present on the surface of OMVs. One application for this approach is the development of vaccines against addictive drugs.

From as early as the 1970's, researchers have been attempting to create vaccines against addictive drugs such as caffeine, morphine, cocaine, and methamphetamine[124-129]. The approaches taken in these studies have been similar to those taken by researchers developing glycoconjugate vaccines in that they have been chemically conjugating these small molecule drugs to strongly immunogenic proteins such as cholera toxin B[130], EPA[131], and OmpC from *N*. *meningitidis*[126]. More modern approaches have used protein-based nanoparticles as carrier proteins including adenovirus[129] and peptide nanofibers[127].

One study compared the immune response to methamphetamine (MA) conjugated to ovalbumin (OVA), keyhole limpet hemocyanin (KLH), tetanus toxoid (TT), and OmpC[126]. In the study, they found that MA specific IgG titers were highest in mice immunized with the MA-OmpC glycoconjugate. The researchers hypothesized that this may be due to residual LPS that is co-purified with OmpC[132]. Looking back with the knowledge of OMV biology and armed with the co-delivery hypothesis, we hypothesize that these researchers were actually immunizing mice with MA conjugated to OmpC embedded in OMVs from *N. meningitidis*.

The researchers tested their hypothesis by adding the LPS mimic monophosphorlyated lipid A (MPL) to the other MA protein conjugates. The new formulations with the MPL adjuvant showed an increased MA specific IgG response relative to non-MPL adjuvanted samples, indicating the innate immunostimulatory properties of LPS in OMVs played a role in the success of the MA-OmpC conjugate. However, the MPL formulated protein conjugates still showed significantly lower MA specific titers than the MA-OmpC conjugates. The proposed method of functionalizing azide-linked PNAG OMVs is ideal for an immunization trial using one of these small molecule drugs. The drugs are relatively easy to synthesize and are amenable to functionalization by bioorthogonal chemistry reactive groups. Immunization of mice would allow us to test the hypothesis of cocaine and carbohydrate antigen co-delivery (CocaCoDe) which implies that conjugation to the OMV liposome is crucial for the most effective immunostimulatory effect while also creating a novel vaccine candidate against an addictive drug.

Creation of multivalent OMV vaccines. While glycOMVs displaying the *F. tularensis* O-antigen are protective against lethal challenge with *F. tularensis* and we expect OMVs containing lumenal EPA glycosylated with *F. tularensis* O-antigen to at least as effective in a challenge model, it is possible that neither formulation will induce long term protection against *F. tularensis.* If that is the case, several protein antigens native to *F. tularensis* previously reported to have TCR binding epitopes (GroEL and IglB) could be modified to contain glycosylation sites [92]. These modified antigens can be used as lumenal or outer membrane protein carriers for the O-antigen in OMVs stimulating stronger protection against *F. tularensis*. It should also be possible to formulate glycOMVs decorated with both O-antigen and PNAG, providing a second glycan antigen that may provide additional protection against challenge. These formulations would be examples of multi-subunit OMV vaccines against a single pathogen. Alternatively, it should be possible to create multi-subunit vaccine against more than one pathogen. If glycOMVs displaying *F. tularensis* O-antigen are sufficiently protective against all strains over a long enough period of time, you could load a protein antigen from a second pathogen such as tetanus toxoid into the OMVs, creating a multivalent vaccine against two pathogens.

Use of a twostep glycosylation process for site-specific glycosylation of a target protein with two unique glycans. It has been shown that it is possible to produce glycosylated proteins *in vivo* with near 100% glycosylation site occupancy when using *C. jejuni* PglB as the OST and its cognate optimal acceptor sequon DQNAT [8, 24, 86]. Conversely, it was also shown that a modified sequon of AQNAT has very little to no detectable glycosylation when wild type *C. jejuni* PglB is used as the OST. The DeLisa Research Group has engineered a mutant of *C. jejuni*

PglB ($PglB^{LQ}$) with relaxed acceptor site specificities that can glycosylate both DQNAT and AQNAT sites [8, 86]. The availability of OSTs with different acceptor site preferences enables orthogonal glycosylation schemes. Here we propose to leverage this system through creating an acceptor protein with two different glycosylation sites (DQNAT and AQNAT) and displaying it on OMVs. Under this regime, the DQNAT site can be glycosylated by both wild type PglB and $PglB^{LQ}$ while the AQNAT site is only able to be glycosylated by $PglB^{LQ}$. If wild type PglB was used in the cell producing OMVs and $PglB^{LQ}$ was used in an *in vitro* glycosylation reaction after the OMVs were harvest, it would be possible to create glycoproteins on OMVs with two distinct oligosaccharides at two distinct specific sites.

References:

1. Koff, W.C., et al., *Accelerating Next-Generation Vaccine Development for Global Disease Prevention.* Science, 2013. **340**(6136): p. 1232910.
2. McAleer, W.J., et al., *Human hepatitis B vaccine from recombinant yeast.* Nature, 1984. **307**(5947): p. 178-180.
3. Weintraub, A., *Immunology of bacterial polysaccharide antigens.* Carbohydrate Research, 2003. **338**(23): p. 2539-2547.
4. Jones, C., *Vaccines based on the cell surface carbohydrates of pathogenic bacteria.* Anais Da Academia Brasileira De Ciencias, 2005. **77**(2): p. 293-324.
5. Trotter, C.L., et al., *Optimising the use of conjugate vaccines to prevent disease caused by Haemophilus influenzae type b, Neisseria meningitidis and Streptococcus pneumoniae.* Vaccine, 2008. **26**(35): p. 4434-4445.
6. Frasch, C.E., *Preparation of bacterial polysaccharide-protein conjugates: analytical and manufacturing challenges.* Vaccine, 2009. **27**(46): p. 6468-6470.
7. Szymanski, C.M., et al., *Evidence for a system of general protein glycosylation in Campylobacter jejuni.* Mol Microbiol, 1999. **32**(5): p. 1022-30.
8. Wacker, M., et al., *N-linked glycosylation in Campylobacter jejuni and its functional transfer into E. coli.* Science (New York, NY), 2002. **298**(5599): p. 1790-1793.
9. Feldman, M.F., et al., *Engineering N-linked protein glycosylation with diverse O antigen lipopolysaccharide structures in Escherichia coli.* Proc Natl Acad Sci U S A, 2005. **102**(8): p. 3016-21.
10. Ihssen, J., et al., *Production of glycoprotein vaccines in Escherichia coli.* Microbial Cell Factories, 2010. **9**.
11. Fisher, A.C., et al., *Production of Secretory and Extracellular N-Linked Glycoproteins in Escherichia coli.* Applied and Environmental Microbiology, 2011. **77**(3): p. 871-881.
12. Guarino, C. and M.P. DeLisa, *A prokaryote-based cell-free translation system that efficiently synthesizes glycoproteins.* Glycobiology, 2012. **22**(5): p. 596-601.
13. Chen, D.J., et al., *Delivery of foreign antigens by engineered outer membrane vesicle vaccines.* Proc Natl Acad Sci U S A, 2010. **107**(7): p. 3099-104.
14. Rosenthal, J.A., et al., *Mechanistic insight into the TH1-biased immune response to recombinant subunit vaccines delivered by probiotic bacteria-derived outer membrane vesicles.* PloS One, 2014. **9**(11).
15. Valentine, J.L., et al., *Immunization with Outer Membrane Vesicles Displaying Designer Glycotopes Yields Class-Switched, Glycan-Specific Antibodies.* Cell Chemical Biology, 2016. **23**(6): p. 655-665.
16. Chen, L., et al., *Outer membrane vesicles displaying engineered glycotopes elicit protective antibodies.* Proceedings of the National Academy of Sciences of the United States of America, 2016. **113**(26): p. E3609-3618.
17. Kulp, A. and M.J. Kuehn, *Biological Functions and Biogenesis of Secreted Bacterial Outer Membrane Vesicles.* Annual Review of Microbiology, 2010. **64**(1): p. 163-184.
18. Hoebe, K., E. Janssen, and B. Beutler, *The interface between innate and adaptive immunity.* Nature Immunology, 2004. **5**(10): p. 971-974.
19. Iwasaki, A. and R. Medzhitov, *Regulation of adaptive immunity by the innate immune system.* Science (New York, N.Y.), 2010. **327**(5963): p. 291-295.
20. Pashine, A., N.M. Valiante, and J.B. Ulmer, *Targeting the innate immune response with improved vaccine adjuvants.* Nature Medicine, 2005. **11**: p. S63-S68.

21. Samuel, G. and P. Reeves, *Biosynthesis of O-antigens: genes and pathways involved in nucleotide sugar precursor synthesis and O-antigen assembly.* Carbohydrate Research, 2003. **338**(23): p. 2503-2519.
22. Kowarik, M., et al., *Definition of the bacterial N-glycosylation site consensus sequence.* The EMBO journal, 2006. **25**(9): p. 1957-1966.
23. Chen, M.M., K.J. Glover, and B. Imperiali, *From peptide to protein: comparative analysis of the substrate specificity of N-linked glycosylation in C. jejuni.* Biochemistry, 2007. **46**(18): p. 5579-5585.
24. Fisher, A.C., et al., *Production of secretory and extracellular N-linked glycoproteins in Escherichia coli.* Appl Environ Microbiol, 2011. **77**(3): p. 871-81.
25. Valderrama-Rincon, J.D., et al., *An engineered eukaryotic protein glycosylation pathway in Escherichia coli.* Nature Chemical Biology, 2012. **8**(5): p. 434-436.
26. Ihssen, J., et al., *Increased efficiency of Campylobacter jejuni N-oligosaccharyltransferase PglB by structure-guided engineering.* Open Biology, 2015. **5**(4).
27. Ihssen, J., et al., *Structural insights from random mutagenesis of Campylobacter jejuni oligosaccharyltransferase PglB.* BMC Biotechnology, 2012. **12**(1): p. 1-13.
28. Wacker, M., et al., *Prevention of Staphylococcus aureus Infections by Glycoprotein Vaccines Synthesized in Escherichia coli.* Journal of Infectious Diseases, 2014. **209**(10): p. 1551-1561.
29. Kelly, J., et al., *Biosynthesis of the N-Linked Glycan in Campylobacter jejuni and Addition onto Protein through Block Transfer.* Journal of Bacteriology, 2006. **188**(7): p. 2427-2434.
30. Lautwein, A., et al., *Inflammatory stimuli recruit cathepsin activity to late endosomal compartments in human dendritic cells.* European Journal of Immunology, 2002. **32**(12): p. 3348-3357.
31. Janeway, J.C.A., Travers, P., Walport, M., and Shlomichik, M. J., *Immunobiology*. 5 ed. 2001, New York: Garland Science.
32. Joffre, O.P., et al., *Cross-presentation by dendritic cells.* Nature Reviews. Immunology, 2012. **12**(8): p. 557-569.
33. Blanchard, N. and N. Shastri, *Cross-presentation of peptides from intracellular pathogens by MHC class I molecules.* Annals of the New York Academy of Sciences, 2010. **1183**: p. 237-250.
34. Ackerman, A.L., A. Giodini, and P. Cresswell, *A Role for the Endoplasmic Reticulum Protein Retrotranslocation Machinery during Crosspresentation by Dendritic Cells.* Immunity, 2006. **25**(4): p. 607-617.
35. Sebastian, S., et al., *Cellular and humoral immunity are synergistic in protection against types A and B Francisella tularensis.* Vaccine, 2009. **27**(4): p. 597-605.
36. Avci, F.Y., et al., *A mechanism for glycoconjugate vaccine activation of the adaptive immune system and its implications for vaccine design.* Nature Medicine, 2011. **17**(12): p. 1602-1609.
37. Avci, F.Y., et al., *Carbohydrates and T cells: a sweet twosome.* Seminars in Immunology, 2013. **25**(2): p. 146-151.
38. Kalka-Moll, W.M., et al., *Zwitterionic polysaccharides stimulate T cells by MHC class II-dependent interactions.* Journal of Immunology (Baltimore, Md.: 1950), 2002. **169**(11): p. 6149-6153.
39. Cobb, B.A. and D.L. Kasper, *Characteristics of carbohydrate antigen binding to the presentation protein HLA-DR.* Glycobiology, 2008. **18**(9): p. 707-718.
40. Snapper, C.M. and J.J. Mond, *A model for induction of T cell-independent humoral immunity in response to polysaccharide antigens.* Journal of Immunology (Baltimore, Md.: 1950), 1996. **157**(6): p. 2229-2233.
41. Vos, Q., et al., *B-cell activation by T-cell-independent type 2 antigens as an integral part of the humoral immune response to pathogenic microorganisms.* Immunological Reviews, 2000. **176**: p. 154-170.

42. Beveridge, T.J., *Structures of Gram-Negative Cell Walls and Their Derived Membrane Vesicles.* Journal of Bacteriology, 1999. **181**(16): p. 4725-4733.
43. Kesty, N.C. and M.J. Kuehn, *Incorporation of heterologous outer membrane and periplasmic proteins into Escherichia coli outer membrane vesicles.* J Biol Chem, 2004. **279**(3): p. 2069-76.
44. Kesty, N.C., et al., *Enterotoxigenic Escherichia coli vesicles target toxin delivery into mammalian cells.* The EMBO Journal, 2004. **23**(23): p. 4538-4549.
45. Kuehn, M.J. and N.C. Kesty, *Bacterial outer membrane vesicles and the host-pathogen interaction.* Genes & Development, 2005. **19**(22): p. 2645-2655.
46. McBroom, A.J. and M.J. Kuehn, *Release of outer membrane vesicles by gram-negative bacteria is a novel envelope stress response.* Molecular Microbiology, 2007. **63**(2): p. 545-558.
47. Ellis, T.N. and M.J. Kuehn, *Virulence and immunomodulatory roles of bacterial outer membrane vesicles.* Microbiology and Molecular Biology Reviews: MMBR, 2010. **74**(1): p. 81-94.
48. Pierson, T., et al., *Proteomic characterization and functional analysis of outer membrane vesicles of Francisella novicida suggests possible role in virulence and use as a vaccine.* J Proteome Res, 2011. **10**(3): p. 954-67.
49. Bonnington, K.E. and M.J. Kuehn, *Protein selection and export via outer membrane vesicles.* Biochimica et Biophysica Acta (BBA) - Molecular Cell Research, 2014. **1843**(8): p. 1612-1619.
50. McBroom, A.J., et al., *Outer Membrane Vesicle Production by Escherichia Coli Is Independent of Membrane Instability.* Journal of Bacteriology, 2006. **188**(15): p. 5385-5392.
51. Bauman, S.J. and M.J. Kuehn, *Purification of outer membrane vesicles from Pseudomonas aeruginosa and their activation of an IL-8 response.* Microbes and Infection / Institut Pasteur, 2006. **8**(9-10): p. 2400-2408.
52. Ellis, T.N., S.A. Leiman, and M.J. Kuehn, *Naturally produced outer membrane vesicles from Pseudomonas aeruginosa elicit a potent innate immune response via combined sensing of both lipopolysaccharide and protein components.* Infection and Immunity, 2010. **78**(9): p. 3822-3831.
53. Persing, D.H., et al., *Taking toll: lipid A mimetics as adjuvants and immunomodulators.* Trends in Microbiology, 2002. **10**(10 Suppl): p. S32-37.
54. Gorringe, A.R. and R. Pajón, *Bexsero: a multicomponent vaccine for prevention of meningococcal disease.* Human Vaccines & Immunotherapeutics, 2012. **8**(2): p. 174-183.
55. Muralinath, M., et al., *Immunization with Salmonella enterica serovar Typhimurium-derived outer membrane vesicles delivering the pneumococcal protein PspA confers protection against challenge with Streptococcus pneumoniae.* Infect Immun, 2011. **79**(2): p. 887-94.
56. Kim, S.-H., et al., *Structural modifications of outer membrane vesicles to refine them as vaccine delivery vehicles.* Biochimica Et Biophysica Acta, 2009. **1788**(10): p. 2150-2159.
57. Breidenbach, M.A., et al., *Targeted metabolic labeling of yeast N-glycans with unnatural sugars.* Proceedings of the National Academy of Sciences, 2010. **107**(9): p. 3988-3993.
58. Saxon, E. and C.R. Bertozzi, *Cell surface engineering by a modified Staudinger reaction.* Science, 2000. **287**(5460): p. 2007-2010.
59. Prescher, J.A., D.H. Dube, and C.R. Bertozzi, *Chemical remodelling of cell surfaces in living animals.* Nature, 2004. **430**(7002): p. 873-877.
60. Laughlin, S.T. and C.R. Bertozzi, *Metabolic labeling of glycans with azido sugars and subsequent glycan-profiling and visualization via Staudinger ligation.* Nature Protocols, 2007. **2**(11): p. 2930-2944.
61. Breidenbach, M.A., et al., *Targeted metabolic labeling of yeast N-glycans with unnatural sugars.* Proc Natl Acad Sci U S A, 2010. **107**(9): p. 3988-93.
62. Baskin, J.M., et al., *Visualizing enveloping layer glycans during zebrafish early embryogenesis.* Proceedings of the National Academy of Sciences, 2010. **107**(23): p. 10360-10365.

63. Chang, P.V., et al., *Copper-free click chemistry in living animals.* Proceedings of the National Academy of Sciences, 2010. **107**(5): p. 1821-1826.
64. Cohen, A.S., et al., *Real-Time Bioluminescence Imaging of Glycans on Live Cells.* Journal of the American Chemical Society, 2010. **132**(25): p. 8563-8565.
65. Chang, P.V., et al., *A Strategy for the Selective Imaging of Glycans Using Caged Metabolic Precursors.* Journal of the American Chemical Society, 2010. **132**(28): p. 9516-9518.
66. Beatty, K.E., et al., *Live-Cell Imaging of Cellular Proteins by a Strain-Promoted Azide–Alkyne Cycloaddition.* ChemBioChem, 2010. **11**(15): p. 2092-2095.
67. Sletten, E.M. and C.R. Bertozzi, *From Mechanism to Mouse: A Tale of Two Bioorthogonal Reactions.* Accounts of Chemical Research, 2011. **44**(9): p. 666-676.
68. Staudinger, H. and J. Meyer, *Über neue organische Phosphorverbindungen III. Phosphinmethylenderivate und Phosphinimine.* Helvetica Chimica Acta, 1919. **2**(1): p. 635-646.
69. Koenigs, M.B., E.A. Richardson, and D.H. Dube, *Metabolic profiling of Helicobacter pylori glycosylation.* Molecular BioSystems, 2009. **5**(9): p. 909.
70. Horsman, M.E., B.R. Lundgren, and C.N. Boddy, *N-Acetylneuraminic Acid Production in Escherichia coli Lacking N-Acetylglucosamine Catabolic Machinery.* Chemical Engineering Communications, 2016. **203**(10): p. 1326-1335.
71. R. Lundgren, B. and C. N. Boddy, *Sialic acid and N -acyl sialic acid analog production by fermentation of metabolically and genetically engineered Escherichia coli.* Organic & Biomolecular Chemistry, 2007. **5**(12): p. 1903-1909.
72. Lundgren, B., *Metabolic and genetic engineering of Escherichia coli for the production of nonulosonic acid sugars.* Biology - Dissertations, 2010.
73. Kaewsapsak, P., O. Esonu, and D.H. Dube, *Recruiting the Host's Immune System to Target Helicobacter pylori's Surface Glycans.* Chembiochem, 2013. **14**(6): p. 721-726.
74. Clark, E.L., et al., *Development of Rare Bacterial Monosaccharide Analogs for Metabolic Glycan Labeling in Pathogenic Bacteria.* ACS Chemical Biology, 2016. **11**(12): p. 3365-3373.
75. Beloin, C., A. Roux, and J.-M. Ghigo, *Escherichia coli biofilms.* Current Topics in Microbiology and Immunology, 2008. **322**: p. 249-289.
76. Morona, J.K., R. Morona, and J.C. Paton, *Attachment of capsular polysaccharide to the cell wall of Streptococcus pneumoniae type 2 is required for invasive disease.* Proceedings of the National Academy of Sciences, 2006. **103**(22): p. 8505-8510.
77. Finne, J., M. Leinonen, and P.H. Mäkelä, *Antigenic similarities between brain components and bacteria causing meningitis. Implications for vaccine development and pathogenesis.* Lancet (London, England), 1983. **2**(8346): p. 355-357.
78. Karlyshev, A.V., *The Campylobacter jejuni general glycosylation system is important for attachment to human epithelial cells and in the colonization of chicks.* Microbiology, 2004. **150**(6): p. 1957-1964.
79. Sandström, G., *The tularaemia vaccine.* Journal of Chemical Technology & Biotechnology, 1994. **59**(4): p. 315-320.
80. Titball, R.W. and J.F. Petrosino, *Francisella Tularensis Genomics and Proteomics.* Annals of the New York Academy of Sciences, 2007. **1105**(1): p. 98-121.
81. Lu, Z., et al., *Protective B-cell epitopes of Francisella tularensis O-polysaccharide in a mouse model of respiratory tularaemia.* Immunology, 2012. **136**(3): p. 352-360.
82. Fulop, M., et al., *Role of antibody to lipopolysaccharide in protection against low- and high-virulence strains of Francisella tularensis.* Vaccine, 2001. **19**(31): p. 4465-4472.
83. Cuccui, J., et al., *Exploitation of bacterial N-linked glycosylation to develop a novel recombinant glycoconjugate vaccine against Francisella tularensis.* Open biology, 2013. **3**(5).

84. O'Callaghan, D., et al., *Immune responses to hybrid maltose-binding proteins.* Vaccine, 1993. **11**(2): p. 140-142.
85. Bernadac, A., et al., *Escherichia coli tol-pal Mutants Form Outer Membrane Vesicles.* Journal of Bacteriology, 1998. **180**(18): p. 4872-4878.
86. Ollis, A.A., Y. Chai, and M.P. DeLisa, *GlycoSNAP: A High-Throughput Screening Methodology for Engineering Designer Glycosylation Enzymes.* Methods in Molecular Biology (Clifton, N.J.), 2015. **1321**: p. 37-47.
87. Wedekind, J.E., et al., *Refined crystallographic structure of Pseudomonas aeruginosa exotoxin A and its implications for the molecular mechanism of toxicity.* Journal of Molecular Biology, 2001. **314**(4): p. 823-837.
88. Kim, J.-Y., et al., *Engineered bacterial outer membrane vesicles with enhanced functionality.* Journal of Molecular Biology, 2008. **380**(1): p. 51-66.
89. van der Pol, L., M. Stork, and P. van der Ley, *Outer membrane vesicles as platform vaccine technology.* Biotechnology Journal, 2015. **10**(11): p. 1689-1706.
90. Ielmini, M.V. and M.F. Feldman, *Desulfovibrio desulfuricans PglB homolog possesses oligosaccharyltransferase activity with relaxed glycan specificity and distinct protein acceptor sequence requirements.* Glycobiology, 2011. **21**(6): p. 734-742.
91. Jervis, A.J., et al., *Characterization of N-Linked Protein Glycosylation in Helicobacter pullorum.* Journal of Bacteriology, 2010. **192**(19): p. 5228-5236.
92. Valentino, M.D., et al., *Identification of T-cell epitopes in Francisella tularensis using an ordered protein array of serological targets.* Immunology, 2011. **132**(3): p. 348-360.
93. Baba, T., et al., *Construction of Escherichia coli K-12 in-frame, single-gene knockout mutants: the Keio collection.* Molecular Systems Biology, 2006. **2**.
94. Ollis, A.A., et al., *Substitute sweeteners: diverse bacterial oligosaccharyltransferases with unique N-glycosylation site preferences.* Scientific Reports, 2015. **5**.
95. Fisher, A.C. and M.P. DeLisa, *A little help from my friends: quality control of presecretory proteins in bacteria.* J Bacteriol, 2004. **186**(22): p. 7467-73.
96. Lizak, C., et al., *X-ray structure of a bacterial oligosaccharyltransferase.* Nature, 2011. **474**(7351): p. 350-5.
97. Cywes-Bentley, C., et al., *Antibody to a conserved antigenic target is protective against diverse prokaryotic and eukaryotic pathogens.* Proceedings of the National Academy of Sciences of the United States of America, 2013. **110**(24): p. E2209-E2218.
98. Mack, D., et al., *The intercellular adhesin involved in biofilm accumulation of Staphylococcus epidermidis is a linear beta-1,6-linked glucosaminoglycan: purification and structural analysis.* Journal of Bacteriology, 1996. **178**(1): p. 175-183.
99. Wang, X., J.F. Preston, and T. Romeo, *The pgaABCD Locus of Escherichia coli Promotes the Synthesis of a Polysaccharide Adhesin Required for Biofilm Formation.* Journal of Bacteriology, 2004. **186**(9): p. 2724-2734.
100. Kaplan, J.B., et al., *Genes involved in the synthesis and degradation of matrix polysaccharide in Actinobacillus actinomycetemcomitans and Actinobacillus pleuropneumoniae biofilms.* Journal of Bacteriology, 2004. **186**(24): p. 8213-8220.
101. Izano, E.A., et al., *Poly-N-acetylglucosamine mediates biofilm formation and antibiotic resistance in Actinobacillus pleuropneumoniae.* Microbial Pathogenesis, 2007. **43**(1): p. 1-9.
102. Choi, A.H.K., et al., *The pgaABCD Locus of Acinetobacter baumannii Encodes the Production of Poly-β-1-6-N-Acetylglucosamine, Which Is Critical for Biofilm Formation.* Journal of Bacteriology, 2009. **191**(19): p. 5953-5963.

103. Maira-Litrán, T., et al., *Comparative Opsonic and Protective Activities of Staphylococcus aureus Conjugate Vaccines Containing Native or Deacetylated Staphylococcal Poly-N-Acetyl-β-(1-6)-Glucosamine.* Infection and Immunity, 2005. **73**(10): p. 6752-6762.
104. Kelly-Quintos, C., et al., *Characterization of the Opsonic and Protective Activity against Staphylococcus aureus of Fully Human Monoclonal Antibodies Specific for the Bacterial Surface Polysaccharide Poly-N-Acetylglucosamine.* Infection and Immunity, 2006. **74**(5): p. 2742-2750.
105. Cerca, N., et al., *Protection against Escherichia coli infection by antibody to the Staphylococcus aureus poly-N-acetylglucosamine surface polysaccharide.* Proceedings of the National Academy of Sciences of the United States of America, 2007. **104**(18): p. 7528-7533.
106. Gening, M.L., et al., *Synthetic β-(1→6)-Linked N-Acetylated and Nonacetylated Oligoglucosamines Used To Produce Conjugate Vaccines for Bacterial Pathogens.* Infection and Immunity, 2010. **78**(2): p. 764-772.
107. Skurnik, D., et al., *Animal and human antibodies to distinct Staphylococcus aureus antigens mutually neutralize opsonic killing and protection in mice.* The Journal of Clinical Investigation, 2010. **120**(9): p. 3220-3233.
108. Skurnik, D., et al., *Natural Antibodies in Normal Human Serum Inhibit Staphylococcus aureus Capsular Polysaccharide Vaccine Efficacy.* Clinical Infectious Diseases: An Official Publication of the Infectious Diseases Society of America, 2012. **55**(9): p. 1188-1197.
109. Vuong, C., et al., *A Crucial Role for Exopolysaccharide Modification in Bacterial Biofilm Formation, Immune Evasion, and Virulence.* Journal of Biological Chemistry, 2004. **279**(52): p. 54881-54886.
110. Cerca, N., et al., *Molecular Basis for Preferential Protective Efficacy of Antibodies Directed to the Poorly Acetylated Form of Staphylococcal Poly-N-Acetyl-β-(1-6)-Glucosamine.* Infection and Immunity, 2007. **75**(7): p. 3406-3413.
111. Korsholm, K.S., et al., *T-helper 1 and T-helper 2 adjuvants induce distinct differences in the magnitude, quality and kinetics of the early inflammatory response at the site of injection.* Immunology, 2010. **129**(1): p. 75-86.
112. Pozzi, C., et al., *Opsonic and Protective Properties of Antibodies Raised to Conjugate Vaccines Targeting Six Staphylococcus aureus Antigens.* PLoS ONE, 2012. **7**(10).
113. Bröker, B.M., D. Mrochen, and V. Péton, *The T Cell Response to Staphylococcus aureus.* Pathogens (Basel, Switzerland), 2016. **5**(1).
114. Brown, A.F., et al., *Memory Th1 Cells Are Protective in Invasive Staphylococcus aureus Infection.* PLOS Pathogens, 2015. **11**(11): p. e1005226.
115. McKenney, D., et al., *The ica Locus of Staphylococcus epidermidis Encodes Production of the Capsular Polysaccharide/Adhesin.* Infection and Immunity, 1998. **66**(10): p. 4711-4720.
116. Chow, S.-C., J. Shao, and H. Wang, *Sample Size Calculations in Clincial Research*. CRC Biostatistics Series. 2008: Chapman and Hall.
117. Yakandawala, N., et al., *Enhanced expression of engineered ACA-less beta-1, 6-N-acetylglucosaminidase (dispersin B) in Escherichia coli.* Journal of Industrial Microbiology & Biotechnology, 2009. **36**(10): p. 1297-1305.
118. Maira-Litrán, T., et al., *Immunochemical Properties of the Staphylococcal Poly-N-Acetylglucosamine Surface Polysaccharide.* Infection and Immunity, 2002. **70**(8): p. 4433-4440.
119. Bradford, M.M., *A rapid and sensitive method for the quantitation of microgram quantities of protein utilizing the principle of protein-dye binding.* Analytical biochemistry, 1976. **72**(1-2): p. 248-254.
120. Sun, H., et al., *Induction of systemic and mucosal immunity against methicillin-resistant Staphylococcus aureus infection by a novel nanoemulsion adjuvant vaccine.* International Journal of Nanomedicine, 2015: p. 7275.

121. Sebastian, S., et al., *A Defined O-Antigen Polysaccharide Mutant of Francisella tularensis Live Vaccine Strain Has Attenuated Virulence while Retaining Its Protective Capacity.* Infection and Immunity, 2007. **75**(5): p. 2591-2602.
122. Boyd, M.A., et al., *Serum Bactericidal Assays To Evaluate Typhoidal and Nontyphoidal Salmonella Vaccines.* Clinical and Vaccine Immunology : CVI, 2014. **21**(5): p. 712-721.
123. Rejman, J., et al., *Size-dependent internalization of particles via the pathways of clathrin- and caveolae-mediated endocytosis.* Biochemical Journal, 2004. **377**(Pt 1): p. 159-169.
124. Berkowitz, B. and S. Spector, *Evidence for active immunity to morphine in mice.* Science (New York, N.Y.), 1972. **178**(4067): p. 1290-1292.
125. Bonese, K.F., et al., *Changes in heroin self-administration by a rhesus monkey after morphine immunisation.* Nature, 1974. **252**(5485): p. 708-710.
126. Kosten, T., et al., *Vaccines against stimulants: cocaine and MA.* British Journal of Clinical Pharmacology, 2014. **77**(2): p. 368-374.
127. Rudra, J.S., et al., *Suppression of Cocaine-Evoked Hyperactivity by Self-Adjuvanting and Multivalent Peptide Nanofiber Vaccines.* ACS Chemical Neuroscience, 2016. **7**(5): p. 546-552.
128. Haney, M., et al., *Cocaine-specific antibodies blunt the subjective effects of smoked cocaine in humans.* Biological Psychiatry, 2010. **67**(1): p. 59-65.
129. Koob, G., et al., *Anti-cocaine vaccine based on coupling a cocaine analog to a disrupted adenovirus.* CNS & neurological disorders drug targets, 2011. **10**(8): p. 899-904.
130. Martell, B.A., et al., *Vaccine Pharmacotherapy for the Treatment of Cocaine Dependence.* Biological Psychiatry, 2005. **58**(2): p. 158-164.
131. Hatsukami, D.K., et al., *Safety and immunogenicity of a nicotine conjugate vaccine in current smokers.* Clinical Pharmacology & Therapeutics, 2005. **78**(5): p. 456-467.
132. Pérez-Cruz, C., et al., *Outer-Inner Membrane Vesicles Naturally Secreted by Gram-Negative Pathogenic Bacteria.* PloS One, 2015. **10**(1).